

1 **Spatial gradients in the characteristics of soil-carbon fractions are associated with abiotic**
2 **features, but not microbial communities**

3

4 Aditi Sengupta^{1*}, Julia Indivero², Cailene Gunn², Malak M. Tfaily^{3,4}, Rosalie K. Chu⁴, Jason
5 Toyoda⁴, Vanessa L. Bailey¹, Nicholas D. Ward^{2,5}, James C. Stegen¹

6 1. Biological Sciences Division, Pacific Northwest National Laboratory, PO Box 999
7 MSIN: J4-18, Richland, WA 99352

8 2. Marine Sciences Laboratory, Pacific Northwest National Laboratory, 1529 West Sequim
9 Bay Road, Sequim, WA 98382

10 3. Department of Soil, Water, and Environmental Sciences, University of Arizona, Tucson,
11 AZ 85719

12 4. Environmental Molecular Sciences Laboratory, Pacific Northwest National Laboratory,
13 Richland, WA 99352

14 5. School of Oceanography, University of Washington, Seattle, WA 98195

15 Correspondence to: aditi.sengupta@pnnl.gov

16

17

18

19

20

21

22

23

24

25 **Abstract**

26 Coastal terrestrial-aquatic interfaces (TAIs) are dynamic zones of biogeochemical cycling
27 influenced by salinity gradients. However, there is significant heterogeneity in salinity influences
28 on TAI soil biogeochemical function. This heterogeneity is perhaps related to unrecognized
29 mechanisms associated with carbon (C) chemistry and microbial communities. To investigate
30 this potential, we evaluated hypotheses associated with salinity-associated shifts in organic C
31 thermodynamics, biochemical transformations, and nitrogen-, phosphorus-, and sulfur-containing
32 heteroatom organic compounds in a first-order coastal watershed in the Olympic Peninsula of
33 Washington state, USA. In contrast to our hypotheses, thermodynamic favorability of water
34 soluble organic compounds in shallow soils decreased with increasing salinity ($43\text{-}867\ \mu\text{S cm}^{-1}$),
35 as did the number of inferred biochemical transformations and total heteroatom content. These
36 patterns indicate lower microbial activity at higher salinity that is potentially constrained by
37 accumulation of less favorable organic C. Furthermore, organic compounds appeared to be
38 primarily marine/algal-derived in forested floodplain soils with more lipid-like and protein-like
39 compounds, relative to upland soils that had more lignin-, tannin-, and carbohydrate-like
40 compounds. Based on a recent simulation-based study, we further hypothesized a relationship
41 between C chemistry and ecological assembly processes governing microbial community
42 composition. Null modelling revealed that differences in microbial community composition—
43 assayed using 16S rRNA gene sequencing—were primarily the result of limited exchange of
44 organisms among communities (i.e., dispersal limitation). This results in unstructured
45 demographic events that cause community composition to diverge stochastically, as opposed to
46 divergence in community composition being due to deterministic selection-based processes
47 associated with differences in environmental conditions. The strong influence of stochastic
48 processes was further reflected in there being no statistical relationship between community

49 assembly processes (e.g., the relative influence of stochastic assembly processes) and C
50 chemistry (e.g., heteroatom content). This suggests that microbial community composition does
51 not have a mechanistic or causal linkage to C chemistry. The salinity-associated gradient in C
52 chemistry was, therefore, likely influenced by a combination of spatially-structured inputs and
53 salinity-associated metabolic responses of microbial communities that were independent of
54 community composition. We propose that impacts of salinity on coastal soil biogeochemistry
55 need to be understood in the context of C chemistry, hydrologic/depositional dynamics, and
56 microbial physiology, while microbial composition may have less influence.

57

58 **1. Introduction**

59 The interface between terrestrial and aquatic ecosystems represent a dynamic and poorly
60 understood component of the global carbon (C) cycle, particularly along the tidally-influenced
61 reaches of coastal watersheds where terrestrial and marine biospheres intersect (Krauss et al.,
62 2018; Neubauer et al., 2013a; Tank et al., 2018; Ward et al., 2017b). Moreover, the nutrient
63 cycles occurring at these terrestrial-aquatic interfaces (TAIs) influence locally important
64 ecosystem services like contaminant fate and transport and water quality (Conrads and Darby,
65 2017; Vidon et al., 2010). While coastal soil C stocks are being increasingly quantified (Hinson
66 et al., 2017; Holmquist et al., 2018; Krauss et al., 2018), the impact of tidally-driven salinity
67 gradients on molecular level features of the soil-C pool and the processes driving soil organic
68 matter (OM) cycling are poorly studied (Barry et al., 2018; Hoitink et al., 2009; Sawakuchi et al.,
69 2017; Ward et al., 2017b). This is particularly true in settings with low freshwater inputs that
70 allows for significant seawater intrusion compared to large river systems (Hoitink and Jay,
71 2016).

72 While multiple processes impact TAI carbon pools (e.g., tidal-inputs, *in situ* root exudates and
73 litter inputs, decomposition processes), there is some indication that microbial diversity and
74 composition impact soil C storage and mineralization (Mau et al., 2015; Trivedi et al., 2016).
75 This points to the intriguing possibility that processes governing microbial community assembly
76 may be associated with OM chemistry, but evaluations of such associations are lacking. This
77 lack of mechanistic knowledge combined with significant ecosystem heterogeneity in
78 biogeochemical function across salinity gradients (more below), highlights a need to understand
79 how molecular-level processes vary with seawater exposure along coastal TAIs. Doing so will
80 help enhance predictive models of TAI biogeochemistry that can be potentially included in
81 ecosystem models to more accurately represent the role of TAIs in the broader Earth system
82 (U.S. DOE., 2017).

83
84 Modeling of coastal TAIs is currently impeded by poor knowledge of the mechanisms
85 underlying salinity-driven variation in biogeochemical function of associated soils. Previous
86 studies have evaluated function primarily as carbon dioxide (CO₂) and methane (CH₄) flux
87 measurements from soil, and/or soil OM concentrations measured as bulk soil C, percent OM
88 and porewater dissolved organic C (DOC) concentrations in large scale coastal plain river
89 systems. Results from field-based natural salinity gradient studies, long-term field manipulations
90 of salinity exposure, and lab-based incubation studies subjecting soils to varying levels of
91 salinity broadly show the following trends: increases in CO₂ and decreases in CH₄ emissions in
92 freshwater soils exposed to increasing salinity (Chambers et al., 2011, 2013, 2014; Liu et al.,
93 2017; Marton et al., 2012; Neubauer et al., 2013a; Steinmuller and Chambers, 2018; Weston et
94 al., 2006, 2011), and negative relationships between salinity and emissions of both CO₂ and CH₄
95 from soils with a history of exposure to high salinity (Chambers et al., 2013; Herbert et al., 2018;

96 Neubauer et al., 2005, 2013a; Weston et al., 2014) (also see Table S1). Exceptions have been
97 observed where CO₂ emissions decreased in historically freshwater coastal wetland soils exposed
98 to seawater (Ardón et al., 2018; Herbert et al., 2018), with Ardón et al. (2018) also reporting an
99 increase in CH₄ flux with salinity and Steinmuller and Chambers (2018) reporting no change in
100 CH₄ flux with increasing salinity. These observations suggest that microbial activity usually
101 increases with salinity in soils that were not previously exposed to saline conditions, while
102 simultaneously indicating reduced microbial activity with increasing salinity in soils that have a
103 historical exposure to high salinity. In contrast to relatively consistent responses of gas fluxes to
104 changes in salinity, there are strong inconsistencies in DOC responses, including no change
105 (Weston et al., 2006, 2011, 2014), increased DOC (Chambers et al., 2014; Tzortziou et al.,
106 2011), and decreased DOC (Ardón et al., 2016, 2018; Liu et al., 2017; Yang et al., 2018) with
107 increasing salinity.

108
109 Relatively consistent gas flux responses to changes in salinity combined with inconsistent DOC
110 responses to elevated salinity suggests decoupling between biogeochemical rates and the
111 concentration of DOC. This apparent decoupling between the size of the C pool (in this case the
112 concentration of DOC) and microbial activity suggests that C biogeochemistry is influenced by
113 salinity-exposure history, which in turn influences nutrient resources available to soil microbial
114 communities. Specifically, any systematic shifts in soil organic carbon (SOC) chemistry (along
115 salinity gradients) that cannot be observed with bulk C measurements (e.g., changes in chemistry
116 that reduce C bioavailability; Neubauer et al. 2013) may result in unpredictable carbon fluxes.
117 Moreover, bulk C content can show no change across gradients of salinity (Neubauer et al.,
118 2013a) and may fail to capture an integrated view of microbially driven C cycling dynamics at
119 TAIs. In contrast, detailed molecular-level evaluation of SOC composition can provide a more

120 mechanistic view of OC transformations, relative to bulk measures of C content or gas flux
121 measurements.
122
123 Despite its potential importance, a detailed understanding of the characteristics of soil organic
124 compounds (Zark and Dittmar, 2018) and their association with microbial communities in
125 coastal TAIs is currently not available. Nonetheless, we derived a series of expectations by first
126 recognizing that (1) our study system is a historically freshwater system, only recently being
127 exposed to salt water due to removal of a culvert in 2014 (see Methods), and (2) microbial
128 activity increases with increasing salinity in historically freshwater systems (Nyman and
129 Delaune, 1991; Smith et al., 1983; Tzortziou et al., 2011). In addition, it is generally expected
130 that microbes preferentially degrade compounds with higher nominal oxidation states (NOSC) or
131 lower Gibbs Free Energy (ΔG^0_{Cox}) due to greater thermodynamic favorability (Boye et al., 2017;
132 Graham et al., 2017, 2018, Stegen et al., 2018, Ward et al., 2017a). An important caveat is that
133 factors such as redox state, physical protection, mineral associations, and microbial community
134 composition can alter this pure chemistry-based expectation (Schmidt et al., 2011). As a simple
135 point of departure, however, we assume that OM reactivity follows NOSC, thereby leading to
136 our first expectation/hypothesis: the average ΔG^0_{Cox} of OM will increase with increasing salinity
137 as organic compounds with greater thermodynamic favorability are preferentially depleted
138 (LaRowe and Van Cappellen, 2011) due to microbial activity increasing with salinity. To
139 develop our second hypothesis we note that actively growing microbial communities are known
140 to enhance biochemical transformations and generate heteroatom containing organic molecules
141 [sulfur (S), nitrogen (N) and phosphorus (P)] (Guillemette et al., 2018; Koch et al., 2014;
142 Ksionzek et al., 2016); therefore greater heteroatom content and more biochemical
143 transformations are expected with increasing salinity. Our third hypothesis is based on

144 microorganisms adapting to saline conditions through the production or sequestration of
145 osmolytes (Gouffi et al., 1999b, 1999a; Sleator and Hill, 2002), a strategy that may require
146 microbes to break down organic molecules to extract N (i.e., N mining). We therefore
147 hypothesize increases in N-containing biochemical transformation with increasing salinity. Our
148 fourth hypothesis is based on the observation that soils in saturated environments like floodplains
149 are expected to be less oxygenated and can also receive deposition of marine/algal derived OM
150 and suspended sediments during tidal flooding. These factors can result in OM having lower
151 oxygen to carbon (O/C) and higher hydrogen to carbon (H/C) ratios as compared to upland soils
152 (Seidel et al., 2016; Tfaily et al., 2014; Ward et al., 2019b). We therefore hypothesize a greater
153 relative abundance of lipid- and protein-like and less lignin- and tannin-like compounds in the
154 floodplain soils, relative to upland (i.e., drained) soil.

155 While we expect systematic shifts in C chemistry across landscape scale salinity gradients, an
156 open question is the degree to which C chemistry is associated with ecological assembly
157 processes governing composition of microbial communities. Soil microorganisms transform soil
158 C, but there is limited evidence of direct links between microbial community assembly processes
159 and molecular-level soil C chemistry (Kubartová et al., 2015; Rocca et al., 2015; Trivedi et al.,
160 2016; van der Wal et al., 2015). Assembly processes, broadly divided into deterministic
161 (systematic impacts of selection) and stochastic (unstructured demographic events) factors,
162 function over space and time to influence the composition of microbial communities, which in
163 turn mediate biogeochemical cycles (Graham et al., 2016, 2017b; Nemergut et al., 2013a; Stegen
164 et al., 2015). [Deterministic processes lead to selection of microbial communities resulting from
165 different organisms having different levels of fitness for a given set of environmental conditions
166 including abiotic variables and biotic factors related to organismal interactions while stochastic
167 processes include random birth/death events and unstructured dispersal.](#) The relative influences

168 of stochastic and deterministic processes can be inferred from phylogenetic distances among
169 microbial taxa using ecological null models. This approach has been widely employed to
170 understand community assembly processes in surface and subsurface microbial ecology (Caruso
171 et al., 2011; Dini-Andreote et al., 2015; Graham et al., 2017a, 2018; Sengupta et al., 2019;
172 Stegen et al., 2012). Furthermore, a recent study used ecological simulation modeling to show
173 that communities experiencing increased rates of dispersal are linked to reduced biogeochemical
174 functioning (Graham and Stegen, 2017). This, combined with evidence of increasing microbial
175 activity with increasing salinity (discussed above) leads to a fifth hypothesis that the influence of
176 deterministic selection will progressively increase with salinity due to increased microbial
177 activity.

178
179 Analyses of specific chemical biomarkers such as lignin phenols, amino acids, and lipids have
180 been used in soils, sediments, and water to quantitatively evaluate the provenance of terrestrial-
181 derived OM (Hedges et al., 1997), the reactivity of OM as it travels through a soil column (Shen
182 et al., 2015), and microbial community composition (Langer and Rinklebe, 2009), respectively.
183 While biomarkers provide quantitative details on OC cycling, they generally represent a small
184 fraction of the total OM pool, thus, non-targeted approaches such as analysis of thousands of
185 organic molecules via Fourier Transform Ion Cyclotron Resonance Mass Spectrometry (FTICR-
186 MS) have become increasingly widespread for determining molecular-level organic compound
187 signatures (Rivas-Ubach et al., 2018) across a variety of terrestrial (Bailey et al., 2017; Simon et
188 al., 2018), aquatic/marine (Lechtenfeld et al., 2015), and transitional settings such as hyporheic
189 zones (Graham et al., 2017a, Stegen et al., 2016, 2018) and river-ocean gradients (Medeiros et
190 al., 2015).

191 The objective of the current study was to test the following hypotheses in a coastal forested
192 floodplain and adjacent upland forest: (1) mean Gibbs Free Energy of organic compounds will
193 increase with increasing salinity; (2 and 3) biochemical transformations, heteroatom content, and
194 N-containing biochemical transformation will increase with increasing salinity; (4) lipid- and
195 protein-like compound classes will be more prevalent in the floodplain soils compared to upland
196 soils in which lignin- and tannin-like molecules will dominate; and (5) microbial community
197 assembly processes will be increasingly deterministic as salinity increases. The chemical forms
198 of C in these soils were characterized using FTICR-MS. We also employed ecological null
199 model analysis to evaluate the relationship between C chemistry and the influences of assembly
200 processes on microbial communities. Based on our results, we propose a conceptual model of
201 organic C processing in a coastal forested floodplain in which landscape-scale gradients in C
202 chemistry are driven by a combination of spatially-structured inputs and salinity-associated
203 metabolic responses of microbial communities that are independent of community composition.

204

205 **2. Materials and Methods:**

206 **2.1 Site Information and Soil Sampling**

207 Soils along a coastal watershed draining a small first order stream, Beaver Creek, in the
208 Washington coast were selected for this study (46.907, -123.976). Beaver Creek is a tributary of
209 Johns River and experiences a high tidal range of up to 2.5 m that extends midway up the first-
210 order stream's channel and inundates the landscape in its floodplains. The confluence of Beaver
211 Creek and Johns River is roughly 2.5 km upstream of the Grays Harbor estuary and 14.5 km
212 from the Pacific Ocean, and experiences variable exposure to saline waters at high tide (Fig. 1).
213 Surface water salinity near Beaver Creek's confluence ranges from 0 practical salinity unit (psu)
214 at low tide to 30 psu at high tide during dry periods (Ward, unpublished). The Beaver Creek

215 watershed is 3.8 km². The tidal floodplain makes up 0.5 km² of this total watershed area. Tidal
216 exchange to Beaver Creek was restored after 2014 when a culvert near the creek's confluence
217 with Johns River was removed (Washington Department of Fish and Wildlife, 2019). Due to the
218 minimal past tidal exchange, the floodplain is dominated by gymnosperm trees (*Picea sitchensis*)
219 that are rapidly dying since the culvert removal (Ward et al., 2019a). The headwaters (before the
220 river channel forms) is a sparsely forested, perennially inundated freshwater wetland with tidal
221 exchange blocked by a beaver dam, followed downstream by a densely forested setting along the
222 river channel. Towards Beaver Creek's confluence salt tolerant grasses such as *Agrostis*
223 *stolonifera* (Creeping bentgrass) become the most dominant land cover as forest cover becomes
224 more sparse. The watershed's hillslope/uplands is dominated by *Tsuga heterophylla* (Western
225 hemlock) trees, but *Picea sitchensis* (Sitka spruce) are also present.

226

227 Two sampling transects perpendicular to the river along the up/downstream salinity gradient
228 were established and represent a high salt exposure site close to the culvert breach location and a
229 moderate salt exposure site upstream of the high salt exposure site. These transects represent a
230 coastal forested wetland with brackish (semi-salty) groundwater and consisted of three terrestrial
231 sampling points at each transect extending from the riparian zone to the beginning of the steep
232 upslope. An additional soil sampling point ~20m uphill from the moderate salt exposure site
233 transect served as a purely terrestrial upland endmember. The soils are Andisols and floodplain
234 transects represented hydric soils classified as Ocosta silty clay loam while the upland site was a
235 well-drained Mopang silt loam. The transects experience periodic inundation episodes which
236 result in surface pooling of tidal water, which can be up to ~1m deep. The water table varies
237 seasonally and during tidal cycles and inundation events, ranging from about 0 to 1m below the
238 ground surface (Ward, unpublished).

239
240 Soil samples were collected in triplicate at each of the seven locations(Fig. 1) [BC2 (2.94 m),
241 BC3 (2.63 m), and BC4 (2.82 m) at the high-salt exposure transect, locations BC12 (2.82 m) ,
242 BC13 (2.67 m), BC14 (3.07 m) at the moderate salt exposure transect, and BC15 (13.45 m) as
243 upland site]. The high-salt exposure transect was 230 m from the moderately saline transect (0.6
244 km from the confluence of Beaver Creek with Johns River), and each site at the transect was ~35
245 m apart from the next. Each transect is ~ 90 m. For data comparison's sake, we classify BC2,
246 BC3, BC12, and BC13 as **floodplain** sites while BC4 and BC14 are further **inland** and ~75 m
247 away from the creek at the base of the densely wooded hillslope. Soil samples for molecular
248 characterization studies were collected at two depths—shallow (10 cm) and deep (19-30 cm).
249 Samples were collected from the face of soil pits using custom mini-corers, placed into sterile
250 amber glass vials, purged with N₂ to maintain anaerobic conditions, frozen in the field within an
251 hour at -20 °C, and stored at -80 °C on return to the lab. Bulk samples were collected for soil
252 physicochemical characterization including texture classification with hydrometer method after
253 organic matter removal, dry combustion with direct measure of total C, nitrogen (N) and sulfur
254 (S) by Elementar Macro Cube, plant-available N as ammonium-nitrogen (NH₄-N) and nitrate-
255 nitrogen (NO₃-N) with 2M KCl quantified on [Lachat QuikChem 8500 Series 2 \(Hach, Loveland](#)
256 [Colorado](#)) as colorimetric reaction, pH measured as 1:2 soil:water slurry measured with Hanna
257 benchtop meter, specific conductivity measured as 1:5 soil:water slurry measured on MP-6p
258 portable specific conductivity meter, gravimetric water content measured after drying soils at
259 105 °C for 48 hours, and bulk density and porosity measured as per standard methods
260 (Sumner,1999). Soil chemical characterization was performed on air-dried sieved soils.

261

262 **2.2 FTICR-MS solvent extraction and data acquisition**

263 Soil organic compounds were extracted using a sequential extraction protocol with polar {water
264 (H₂O)} and non-polar {chloroform (CHCl₃) (representing mineral-bound fraction)} solvents per
265 standardized protocols (Graham et al., 2017a; Tfaily et al., 2015, 2017), which extract about 2-
266 15% of total organic carbon and represent both polar and non-polar soil organic carbon fractions.
267 **Importantly, our analyses do not depend on extracting a large portion of the C found within a**
268 **given soil sample. Instead, we assume that the extracted fraction is a representative sub-sample.**
269 This is a standard approach and assumption made in any study examining metabolites or other
270 types of organic molecules in soil. Briefly, extracts were prepared by adding 5 ml of MilliQ H₂O
271 to 5 g of each of the replicate samples in sterile polypropylene centrifuge tubes (Genesee
272 Scientific, San Diego, USA) suitable for organic solvent extractions and shaking for 2 h on a
273 Thermo Scientific LP Vortex Mixer. Samples were removed from the shaker and centrifuged for
274 5 minutes at 6000 rpm, and the supernatant was removed into a fresh centrifuge tube. This step
275 was repeated two more times, with the 15 ml supernatant pooled for each sample and stored at -
276 80 °C until further processing. Next, Folch extraction with CHCl₃ and CH₃OH was performed
277 for each soil pellet left over from the water extraction. Folch extraction entailed adding 2 ml
278 CH₃OH, vortexing for 5 seconds, adding 4 ml CHCl₃, vortexing for 5 seconds, followed by 0.25
279 ml of MilliQ H₂O. The samples were shaken for 1 hr and another 1.25 ml MilliQ H₂O was added
280 and left overnight at 4 °C to obtain bi-layer separation of upper (polar) layer and the lower (non-
281 polar) layer. The extracts were stored in glass vials at -20 °C until ready to be used. The water
282 soluble organic carbon (WSOC) fraction was further purified using a sequential phase extraction
283 (SPE) protocol to remove salts as per Dittmar et al., 2008. Briefly, samples were acidified to pH
284 2 with 85% phosphoric acid. The samples were passed through Bond Elut PPL cartridges
285 (©Agilent Technologies) that were preactivated with CH₃OH. The cartridges were washed 5x
286 with 10mM HCl followed by nitrogen-gas drying. Next, 1.5 ml CH₃OH, a solvent that is

287 compatible with direct analysis on the FTICR-MS, was used to elute the samples from the
288 cartridge thus avoiding an additional evaporation step and reducing the chance of losing volatile
289 organic compounds and saving time during sample preparation. While SPE by PPL have shown
290 not to be very effective in extracting several major classes of DOM compounds that had high ESI
291 efficiencies, such as carboxylic acids and organo-sulfur compounds, and that out-competed other
292 less functionalized compounds (e.g., carbohydrates) for charge in the ESI source (Tfaily et al.,
293 2012), it is highly efficient for marine and estuary DOM samples as it provides complete
294 desalination of the sample. Loss of small molecules such as simple sugars is known to happen
295 during SPE however this is not a concern for the current study as FTICR-MS is sensitive for
296 compounds above 200 Da. In this study, SPE by PPL isolates a major DOM fraction, that is salt-
297 free, allowing for DOM characterization by FTICR-MS(Dittmar et al., 2008b) . While we didn't
298 measure SPE extraction efficiency for this study, it usually ranges between 40 and 62 %
299 depending on the sample (Dittmar et al. 2008). Samples that are collected from the same
300 ecosystem have shown to have similar extraction efficiency. The extracts were injected into a 12
301 Tesla Bruker SolariX FTICR-MS located at Environmental Molecular Sciences Laboratory
302 (EMSL) in Richland, WA, USA. Detailed methods for instrument calibration, experimental
303 conditions, and data acquisition are provided in Graham et al., 2017a and Tfaily et al., 2017.

304

305 **2.3 FTICR-MS Data Processing**

306 One hundred forty-four individual scans were averaged for each sample and internally calibrated
307 using an organic matter homologous series separated by 14 Da ($-\text{CH}_2$ groups). The mass
308 measurement accuracy was less than 1 ppm for singly charged ions across a broad m/z range
309 (100 - 900 m/z). Data Analysis software (Bruker Daltonik version 4.2) was used to convert raw
310 spectra to a list of m/z values applying FTMS peak picker module with a signal-to-noise ratio

311 (S/N) threshold set to 7 and absolute intensity threshold to the default value of 100. Chemical
312 formulae were then assigned using in-house software following the Compound Identification
313 Algorithm, proposed by Kujawinski and Behn (2006), modified by Minor et al. (2012), and
314 described in Tolić et al. (2017). Peaks below 200 and above 900 were dropped to select only for
315 calibrated and assigned peaks. Chemical formulae were assigned based on the following criteria:
316 $S/N > 7$, and mass measurement error < 0.5 ppm, taking into consideration the presence of C, H,
317 O, N, S, P, and excluding other elements. Detected peaks and associated molecular formula were
318 uploaded to the in-house pipeline FTICR R Exploratory Data Analysis (FREDA) to obtain: (i)
319 NOSC values from elemental composition of the organic compounds (Koch and Dittmar, 2006,
320 2016), (ii) thermodynamic favorability of the compounds calculated as Gibbs Free Energy for the
321 oxidation half reactions of the organic compounds (ΔG^0_{Cox}) based on the equation $\Delta G^0_{\text{Cox}} =$
322 $60.3 - 28.5 * \text{NOSC}$ (LaRowe and Van Cappellen, 2011), where a higher ΔG^0_{Cox} indicates a less
323 thermodynamically favorable species than a lower value (LaRowe and Van Cappellen, 2011),
324 (iii) abundance of compounds grouped into elemental groups (CHO, CHOS, CHOP, CHNOS,
325 CHNO, CHNOP, CHOSP, and CHNOSP), and (iv) abundance of compound classes
326 (carbohydrate-, lipid-, protein-, amino sugar-, lignin-, tannin-, condensed hydrocarbon-, and
327 unsaturated hydrocarbon-like) based on molar H:C and O:C ratios of the compounds (Bailey et
328 al., 2017).

329
330 Biochemical transformations potentially occurring in each sample were inferred from the
331 FTICR-MS data by comparing mass differences in peaks within each sample to precise mass
332 differences for commonly observed biochemical transformations (Breitling et al., 2006; Stegen
333 et al., 2018b). The ultra-high mass accuracy of FTICR-MS allows precise mass differences to be

334 counted for the number of times each transformation was observed within each sample. Briefly,
335 the mass difference between m/z peaks extracted from each spectrum were compared to
336 commonly observed mass differences associated with 92 common biochemical transformations
337 provided in previous publications (Graham et al., 2017a; Stegen et al., 2018c). All possible
338 pairwise mass differences were calculated within each extraction type for each sample, as shown
339 in Fig. 2 where a mass difference of 2.01586 indicates a hydrogenation reaction. **It is important**
340 **to note that direct injection electrospray ionization (ESI) FTICR-MS approach cannot distinguish**
341 **between isomers such as in the case of a mass difference corresponding to a loss of grain of**
342 **either glucose, fructose and galactose.**

343

344 **2.4 Ecological Modeling**

345 Null modeling was used to estimate influences of ecological processes on microbial community
346 composition from rarefied (10000) 16S rRNA amplicon data, providing estimates of microbial
347 community composition and phylogenetic relatedness. The extraction, purification, and
348 sequencing of soil microbial DNA were performed according to published protocol (Bottos et al.,
349 2018). Briefly, microbial DNA was extracted from 0.25 g of each sample using the MoBio
350 Power Soil DNA Isolation Kit and cleaned-up using Zymo ZR-96 Genomic DNA Clean and
351 Concentrator-5 kit (Zymo Research Corporation, Irvine, CA) as per manufacturer instructions.
352 The V4 region of the 16S rRNA gene was amplified by polymerase chain reaction and amplicons
353 sequenced on Illumina MiSeq using the 500 Miseq Reagent Kit v2 (Illumina Inc., San Diego,
354 CA) according to manufacturer's instructions. Sequence pre-processing, operational taxonomic
355 unit (OTU) table construction and phylogenetic tree building were performed using an in-house
356 pipeline, HUNDO (Brown et al., 2018). Briefly, sequence demultiplexing was done using EA-
357 Utils (Aronesty, 2013), reads quality filtered with BBDuk2 (BBMap, 2014), and merged using

358 USEARCH (Edgar, 2010). Sequence de-replication and clustering was performed, taxonomy
359 was assigned to operational taxonomic unit (OTU), and chimeras were removed using
360 USEARCH. Raw sequences are archived at NCBI (BioProject PRJNA541992) at the following
361 website:
362 <https://dataview.ncbi.nlm.nih.gov/object/PRJNA541992?reviewer=b55qu29emsinvk3udb2rmuff>
363 qh.

364
365 Null modeling was performed as described previously (Stegen et al., 2013, 2015) with a total of
366 35 samples to estimate relative influences of deterministic and stochastic selection processes.
367 Briefly, samples that passed quality control and rarefaction threshold were evaluated for pairwise
368 phylogenetic turnover between communities, calculated as the difference between the observed
369 values of the β -mean-nearest-taxon-distance (β MNTD) and mean of the null β MNTD
370 distribution, in units of standard deviation (see Stegen et al. 2012 for details). The difference
371 between observed β MNTD and the null distribution is known as the β -nearest taxon index
372 (β NTI). Deterministic assembly process are inferred to be dominant when β NTI > 2 or < -2 .
373 When β NTI is > 2 it indicates that deterministic processes have driven community composition
374 apart, which is referred to as ‘variable selection’ (Dini-Andreote et al. 2015; Stegen et al. 2015).
375 When β NTI is < -2 it indicates that deterministic processes have caused community composition
376 to be similar between a given pair of communities, which is referred to as ‘homogeneous
377 selection’ (Dini-Andreote et al. 2015; Stegen et al. 2015).

378
379 Pairwise community comparisons that do not deviate significantly from the null distribution (i.e.,
380 $2 > \beta$ NTI > -2) indicate the dominance of stochastic processes (including homogenizing dispersal
381 and dispersal limitation), or a scenario in which neither deterministic or stochastic processes

382 dominate (referred to as undominated). Homogenizing dispersal occurs when rate of dispersal
383 between two communities result in community composition becoming relatively similar between
384 the two communities, and potentially overwhelming other assembly processes (e.g., variable
385 selection). Dispersal limitation is the result of very low rates of organismal exchange between
386 communities, which can result in the stochastic divergence of community composition through
387 the accumulated outcomes of random birth/death events (i.e., ecological drift).

388

389 For pairwise comparisons that were not associated with deterministic processes (i.e., when $2 >$
390 $\beta\text{NTI} > -2$), we use a second null model to test for influences of homogenizing dispersal or
391 dispersal limitation. This second null model is referred to as RC_{bray} , and like βNTI accounts for
392 variation in OTU relative abundances (Stegen et al., 2013, 2015). Homogenizing dispersal was
393 inferred to be the dominant process for pairwise comparisons characterized by $2 > \beta\text{NTI} > -2$ and
394 $\text{RC}_{\text{bray}} < -0.95$. Dispersal limitation was inferred to be the dominant process for pairwise
395 comparisons characterized by $2 > \beta\text{NTI} > -2$ and $\text{RC}_{\text{bray}} > 0.95$. The relative influences of variable
396 selection, homogeneous selection, dispersal limitation, and homogenizing dispersal were
397 quantified by the fraction of pairwise comparisons that were dominated by each ecological
398 process (Stegen et al. 2013). The relative contribution of scenarios in which the system was
399 undominated was estimated as the fraction of pairwise comparisons characterized by $2 > \beta\text{NTI} > -$
400 2 and $0.95 > \text{RC}_{\text{bray}} > -0.95$ (Stegen et al. 2015).

401

402 **2.5 Statistical Methods**

403 Samples were separately analyzed for WSOC and CHCl_3 fractions. Within each solvent fraction,
404 samples were grouped into shallow or deep depths. FTICR-MS dependent metrics including
405 ΔG^0_{Cox} , and relative abundance of compound classes, total transformations, nitrogen-containing

406 transformations, and organic nitrogen containing compounds were regressed against specific
407 conductivity. Regressions were considered significant if $R^2 \geq 0.50$ and $p \leq 0.05$. The
408 transformation profiles were also regressed with the community assembly processes to determine
409 the relationship between deterministic/stochastic processes and organic compound
410 transformations. Mantel tests were used to evaluate similarity between BNTI matrix and
411 Sorensen matrix of peak presence/absence. The Sorensen distance matrices of WSOC and CHCl_3
412 peaks were regressed against measured variables (soil physicochemical properties) and
413 community assembly process-variables to determine correlations. Finally, a redundancy analysis
414 –based stepwise model building with forward model choice was performed to determine
415 variation in the Hellinger-transformed water-fraction peaks and CHCl_3 fraction peaks as
416 explained by explanatory variables (which included measured soil variables, modeled
417 community assembly variables, and categorical variables depth and location). All statistical
418 analyses were performed in the statistical computing language R version 3.5.3 (R Development
419 Core Team, 2019).

420

421 **3. Results**

422 **3.1 Soil characterization.** The percent of total soil C (%C) in the shallow soils ($26.3 \pm 8.3\%$)
423 was higher than the deeper soils ($4.0 \pm 1.3\%$) for the lowland soils (i.e. “floodplain” and “inland”
424 sites), while the upland site had an average %C of $7.4 \pm 0.27\%$ at 10 cm and $2.13 \pm 0.06\%$ at 30
425 cm (Table S2). No significant relation was observed between %C in the shallow inland and
426 floodplain soils along the salinity gradient. The percent of total soil N (%N) of the shallow soils
427 were higher ($1.5 \pm 0.40\%$) than the deeper soils ($0.4 \pm 0.08\%$) for the lowland soils and co-varied
428 with %C ($r^2=0.95$). The pH of all soils were acidic (5.64 ± 0.70). The concentrations of $\text{NH}_4\text{-N}$
429 and $\text{NO}_3\text{-N}$ showed a consistent trend where $\text{NH}_4\text{-N}$ was 1-2 orders of magnitude higher than

430 NO₃-N in all samples. The specific conductivity (used as a measurement of salinity in this study)
431 of the shallow soils ranged from 206-866 (± 12) $\mu\text{S cm}^{-1}$ in the lowland soils to 43 ± 5 $\mu\text{S cm}^{-1}$ in
432 the terrestrial end-member site. The deep soils exhibited specific conductivity ranging from to
433 148-524 (± 11) $\mu\text{S cm}^{-1}$ in the lowland soils to 29.2 ± 8 $\mu\text{S cm}^{-1}$ in the terrestrial end-member site.
434 Texture analysis revealed a broad range of sand (4.1 – 40 %), silt (21.4 – 57.9%), and clay (28.6
435 – 64.8%) fractions.

436

437 **3.2 Thermodynamics, compound classes, and elemental composition.** The calculated ΔG^0_{Cox}
438 WSOC (Table S3) in shallow soils was consistent with our hypothesis of decreasing
439 thermodynamic favorability with increasing conductivity. Average ΔG^0_{Cox} ranged from 53-71 kJ
440 mol C⁻¹ ($R^2 = 0.78$, $p < 0.00001$), while no significant relationship between ΔG^0_{Cox} and specific
441 conductivity was observed for WSOC fraction in the deeper soils (averaging 51-54 kJ mol C⁻¹)
442 for the floodplain and inland samples (Fig. 3). The upland site had significantly higher average
443 ΔG^0_{Cox} (67-70 kJ mol C⁻¹) than the soils near the lowland. The ΔG^0_{Cox} (CHCl₃) at both depths
444 (Table S4) was higher than the water fractions (ranging between 96-105 kJ mol C⁻¹) but did not
445 show significant relationship with respect to specific conductivity.

446

447 Peak profiles for each solvent extraction showed distinct compound classes in the van Krevelen
448 space, with peaks assigned to specific compound classes according to rules outlined in Kim et
449 al., 2003 and modified by Bailey et al., 2017. The WSOC fraction was dominated by compounds
450 classified as protein-, amino sugar-, lignin-, condensed hydrocarbon-, carbohydrate-, and tannin-
451 like compounds (Table 1), while the CHCl₃ fraction had relative high abundances (75% and
452 higher) of lipid-like compounds (data not shown). A modest percentage of peaks (11-17%) did
453 not have classes assigned. Unique and common peaks extracted in the WSOC fraction in samples

454 grouped according to their landscape position and depth [four sites in the floodplain (BC2, BC3,
455 BC12, and BC13), two sites inland (BC4 and BC14), and one upland site (BC15)] are
456 represented as H/C to O/C ratio of the compounds ($p = 0.05$) in Fig. S1.

457 The shallow WSOC in the floodplain had greater relative abundance of unique lipid (28%)- and
458 protein (25%)-like compounds with relatively high H:C and low O:C ratios as compared to the
459 upland site (BC15), which had an 31%, 30%, and 19% unique peaks representing lignin-,
460 tannin-, and carbohydrate-like compounds respectively. About 23% of peaks were common in
461 both groups, including lignin- and condensed hydrocarbon-like compounds (Fig. S1a). Between
462 the floodplain and the inland samples, high H:C and low O:C ratios representing 47% lipid-,
463 38% protein-, and 22% amino sugar-like peaks were uniquely present in the floodplain samples
464 (Fig. S1b). The inland shallow soils had 19% unique higher H:C peaks representing condensed
465 hydrocarbon-like compounds compared to 1.2% in the upland soil , though most of the
466 compound classes were observed at both locations (Fig. S1c). Linear regression with specific
467 conductivity profiles showed significant positive correlation with amino sugar-, protein-, lipid-,
468 and unsaturated hydrocarbon-like compounds, while condensed hydrocarbon-like compounds
469 were significantly negatively correlated (Table S5)

470
471 For the deep soils, the upland site had 32% unique peaks with relatively high H:C ratios and low
472 O:C ratios commonly associated with unsaturated hydrocarbon-like compounds, as compared to
473 the 0.7% in the floodplain which had higher prevalence of unique peaks representing condensed
474 hydrocarbon (36%)-, and tannin-like (35%) compounds (Table 1, Fig. S1d). The floodplain vs
475 inland samples had thrice as many unique peaks with high H:C and low O:C ratios representing
476 lipid-like compounds in the floodplain samples. Comparisons between inland and upland end-
477 member samples revealed 43% and 37% unique peaks representing low H:C and high O: C ratio

478 hydrocarbon- and tannin-like compounds respectively in inland samples, while 32%, 14% 9%,
479 and 12% of unique peaks were matched to unsaturated hydrocarbon-, lipid-, protein-, and amino
480 sugar-like compounds respectively in the latter (Table 1, Fig. S1e, f). No significant relationship
481 between compound-class abundances and specific conductivity was observed (Table S5). For the
482 CHCl₃ fraction, peaks of lipid-like and unsaturated hydrocarbon-like compounds were observed
483 to be common in all samples (data not shown) and regressions against specific conductivity were
484 not significant for the compound classes.

485
486 Compositional differences of the organic compounds showed variable heteroatom abundances,
487 with cumulative heteroatom abundance decreasing with increasing salinity ($R^2=0.43$, $p = 0.009$)
488 for shallow fraction of the WSOC. For the WSOC fraction, heteroatom abundance of CHOP (R^2
489 $= 0.61$) and CHNOP ($R^2 = 0.50$) containing compounds was consistent with our hypothesis and
490 significantly ($p < 0.01$) increased, while CHNOS ($R^2 = 0.66$), and CHNOSP ($R^2 = 0.62$)
491 abundances were inconsistent with our hypothesis and significantly decreased with increasing
492 specific conductivity. The elemental composition of the WSOC compounds for deep soils did not
493 show any significant trend with respect to conductivity. For the CHCl₃ fraction, relative
494 abundance of CHNOP in the shallow soils significantly decreased with specific conductivity (R^2
495 $= 0.57$, $p < 0.01$).

496
497 **3.3 Transformation profiles.** In contrast to our expectations, the number of transformations
498 decreased with increasing salinity in the water fraction of shallow soils ($R^2= 0.60$, $p < 0.01$) (Fig.
499 4a, Table S3). We also evaluated N-containing transformations and the abundance of N-
500 containing compounds in the system. Total nitrogen-containing transformations also decreased
501 significantly with conductivity but the correlation was not as strong ($R^2= 0.40$, $p < 0.01$). Total N

502 containing compounds (Fig. 4b, Table S3) as well as their relative abundance decreased
503 significantly ($R^2= 0.74$, $p < 0.01$), with increasing conductivity in the shallow soils for water
504 fraction.

505

506 **3.4 Ecological processes impacting community composition**

507 Null modeling revealed that microbial community assembly processes were influenced by
508 variable selection ($\beta\text{NTI}>2$), homogenous selection ($\beta\text{NTI}<-2$), dispersal limitation ($2>\beta\text{NTI}>-2$
509 and $\text{RC}_{\text{bray}}>0.95$), homogenizing dispersal ($2>\beta\text{NTI}>-2$ and $\text{RC}_{\text{bray}}<-0.95$), and undominated
510 processes ($2>\beta\text{NTI}>-2$ and $0.95>\text{RC}_{\text{bray}}>-0.95$) (Fig. 5). Dispersal limitation had the greatest
511 influence, responsible for 54% of the variation in community composition. The lowest signal
512 was for homogenizing dispersal (1%), and the signal for homogenous selection (23%) was higher
513 than variable selection (9%). Together, deterministic processes (variable selection plus
514 homogeneous selection) were responsible for 32% of the variation in community composition,
515 with 55% contributed by stochastic processes (dispersal limitation plus homogenizing dispersal).
516 Variation not accounted by dispersal or selection (i.e., influenced by a mixture of processes)
517 accounted for the remaining signal (23%). Consistent with influences from both stochastic and
518 deterministic processes, βNTI relationships with environmental variables were significant ($p <$
519 0.05 by Mantel test), but relatively weak ($r=0.46$ for pH and $r=0.31$ for specific conductivity)
520 (Fig. S2).

521

522 To evaluate associations between microbial community assembly processes and chemistry,
523 process estimates were regressed against features of the organic C profiles. Deterministic
524 processes decreased (Fig S3a) while community assembly processes influenced by non-
525 deterministic processes increased with increasing number of transformations of organic

526 compounds (Fig. S3b), although no strong relationships were observed between assembly
527 processes and transformations ($p = 0.027$, $R^2 = 0.11$ for deterministic/non-deterministic
528 processes, $p = 0.475$, $R^2 = 0.015$ for variable selection, $p = 0.054$, $R^2 = 0.10$ for homogenous
529 selection, $p = 0.514$, $R^2 = 0.013$ for dispersal limitation, and $p = 0.627$, $R^2 = 0.007$ for
530 homogenizing dispersal). No significant relationships were observed between assembly
531 processes and the number of N-containing transformations. Sorensen dissimilarity values based
532 on the detected FTICR peaks for the water fraction were correlated with distance matrices of
533 measured environmental variables and estimates of community assembly processes. Weak
534 positive correlations were observed with $\text{NH}_4\text{-N}$ ($r = 0.28$), pH ($r = 0.27$), specific conductivity (r
535 $= 0.41$), $\text{NO}_3\text{-N}$, silt, and clay ($r = 0.30$) while for the CHCl_3 fraction, weak positive correlations
536 were observed with specific conductivity and $\text{NO}_3\text{-N}$ ($r = 0.26$) (Fig. S4). A Mantel test of
537 FTICR Sorensen dissimilarity vs βNTI values yielded a significant relationship ($r = 0.213$, $p =$
538 0.003) for water fraction but not for CHCl_3 fraction ($r=0.076$, $p = 0.152$). The stepwise model
539 building yielded a combination of five variables that were weakly associated with the
540 composition of water fraction peaks ($p=0.026$, adj. $R^2 = 0.217$), including sand, dispersal
541 limitation, $\text{NH}_4\text{-N}$ concentration, specific conductivity, and location. The model explaining
542 variation in the composition of CHCl_3 fraction peaks was non-significant ($p = 0.1$, adj. $R^2 =$
543 0.05).

544

545 **4. DISCUSSION**

546 Sea level rise is increasing the inland extent of tides and exacerbating storm surge, resulting in
547 greater salinity intrusion and altered ecosystem behavior across coastal TAIs (Conrads and
548 Darby, 2017; Ensign and Noe, 2018; Langston et al., 2017; McCarthy et al., 2018; Neubauer et
549 al., 2013b). Site-driven variations in the responses of bulk soil biogeochemical processes (i.e.,

550 gas flux and DOC release) to elevated salinity suggests potentially important influences of
551 underlying features such as C chemistry and microbial communities. To provide a foundation for
552 understanding the role of C chemistry and microbial communities on biogeochemical cycling in
553 coastal soils, we evaluated associations among a landscape-scale soil salinity gradient,
554 molecular-level soil carbon chemistry, and microbial community assembly processes in order to
555 ultimately inform future improvements for predictive models. In soils associated with a coastal
556 first-order drainage basin, we observed salinity-associated gradients in soil organic carbon
557 fractions that were not associated with microbial community assembly processes. Our results are
558 consistent with C chemistry being driven by a combination of spatially-structured inputs driven
559 by landscape structure (i.e., terrestrial inputs further inland, marine inputs further downstream)
560 and salinity-associated metabolic responses of microbial communities that are independent of
561 microbial community composition. An important caveat is that we did not measure microbial
562 metabolism, but instead infer an influence of microbial metabolism due to microbial composition
563 being independent of C chemistry. To more directly evaluate these inferences, additional work is
564 needed that focuses on quantifying inputs (e.g., via stable isotopes) and measuring microbial
565 metabolism (e.g., via metatranscriptomics). Future work should also use tools like Nuclear
566 Magnetic Resonance and Gas Chromatograph-Mass Spectrometry to evaluate low molecular
567 weight OC (like those contributed by root exudates) vary with salinity.

568

569 **4.1 Molecular characterization reveals chemical gradients not seen in the bulk C pool**

570 The systematic shifts observed in the molecular signatures compared to non-significant changes
571 in bulk C chemistry shows that molecular-level investigations are particularly relevant to
572 process-based resolution of C biogeochemistry. The absence of bulk C signals mimicking
573 molecular C signals parallel studies indicating rapid change in molecular constituents of the soil

574 C pool with no change in gross C content (Graham et al., 2018; Reynolds et al., 2018). A faster
575 turnover time of C has been observed in microbial biomass as compared to bulk soil organic
576 matter (Kramer and Gleixner, 2008), which is likely to impact microbe-mediated biochemical C
577 transformations and lead to chemically complex heterogeneous C signatures likely to be missed
578 in bulk analysis (Tfaily et al., 2015). The systematic shifts in chemical characteristics of soil
579 carbon fractions exhibited by samples at the shallow depth suggests that organic C compound
580 pools in shallower soil depths are sensitive to salinity gradients while deeper depth signatures do
581 not vary systematically across the landscape. The landscape gradient observed in the shallow
582 soils is likely influenced by a combination of reduced litterfall due to trees suffering under recent
583 increases in salinity, changing understory vegetation, and algae-rich particulate OM deposition
584 during inundation events that presumably initiated after the recent culvert removal (Wang et. al,
585 2019). In contrast, the deeper soil depths were more similar to older organo-mineral complexed
586 C in terrestrial soils across various ecosystems and land uses (Conant et al., 2011; Dungait et al.,
587 2012; Jobbágy and Jackson, 2000; Kramer and Gleixner, 2006, 2008). The lack of any
588 systematic gradients in the mineral-associated soil C provides further evidence in support of
589 these interpretations, in addition to previous studies showing mineral-associated soil C to be less
590 responsive to environmental forcings, relative to water soluble C (Reynolds et al., 2018).

591

592 **4.2 Decreases in organic C thermodynamic favorability may restrict microbial activity**

593 Consistent with our first hypothesis, systematic changes in chemical characteristics of soil
594 carbon fractions were observed with thermodynamically less favorable C present at high salinity
595 in shallow soils. This gradient was expected to emerge from increased microbial activity at
596 higher salinity leaving behind less favorable organic C. However, decreases in the number of
597 inferred biochemical transformations and heteroatom abundances with increasing salinity

598 suggests that microbial activity decreased with increasing salinity imply (but do not quantify)
599 lower microbial activity at higher salinity. While difficult to infer direction of causality, these
600 patterns suggest that less favorable C at higher salinities may constrain microbial activity,
601 leading to fewer biochemical transformations of the organic C. Thermodynamic limitation of
602 organic C transformation is likely due to anaerobic conditions (LaRowe and Van Cappellen,
603 2011), which are indicated by high-moisture content of soils, high NH₄-N, and low NO₃-N.
604 Anaerobic conditions restrict oxidation of C compounds based on thermodynamic properties
605 (i.e., NOSC and ΔG^0_{Cox}) (Boye et al., 2017), and our data suggest that this has the potential to
606 lead to lower microbial activity in conditions with less favorable organic C.

607

608 **4.3 Compound class landscape gradients suggest influences of spatially structured inputs**

609 Similar to patterns in C thermodynamic favorability, C compound classes showed significant
610 heterogeneity in shallow soils but had conserved characteristics in deeper soils. The lipid-like
611 peaks observed in the shallow floodplain samples suggest marine-associated algal-derived lipid
612 organic matter similar to results observed by Ward et al., 2019 in a coastal wetland setting. In
613 contrast, lignin-like signatures in the upland site suggest terrestrially derived OM, as has been
614 observed in other environments where terrestrially-derived organic molecules have a high
615 abundance of vascular-plant derived material such as lignin (Hedges and Oades, 1997; Ward et
616 al., 2013). These characteristics also align with reports of saturated soil environments (*e.g.*,
617 floodplains) exhibiting greater abundance of less-oxygenated organic matter than aerobic
618 environments (*e.g.*, upland soils) as reported by Tfaily et al., 2014 in organic matter
619 transformation of a peat column. Our observed landscape gradients in compound class
620 composition indicate spatially structured inputs of organic C such as particulate OM deposition
621 (Langley et al., 2007). Combining this outcome with gradients observed in the total number of

622 biochemical transformations and the contribution of heteroatoms suggests that sources of C
623 (marine vs terrestrial) and *in situ* processing combine to influence landscape-scale gradients
624 molecular-level organic C chemistry.

625

626 **4.4 Ecological assembly processes are weakly associated with organic C**

627 Our results show that microbial community assembly is driven by a combination of dispersal
628 limitation (a stochastic process) and deterministic selection most likely associated with pH, as is
629 often observed in soils (Fierer, 2017; Fierer and Jackson, 2006; Garbeva et al., 2004). In contrast,
630 variation in organic C character was associated primarily with specific conductivity. This
631 suggests that the composition of microbial communities is not mechanistically related to C
632 chemistry. Consistent with this inference, we found a very weak association between β NTI and
633 organic C characteristics. Furthermore, and contrary to our hypothesis, we observed a weak
634 negative association between the influence of deterministic processes and the number of organic
635 C transformations.

636

637 Relatively fast changes of organic C chemistry compared to relatively slow changes in microbial
638 composition may underlie the lack of association between assembly processes and C chemistry
639 (Bramucci et al., 2013). Supporting this interpretation, a recent study evaluating microbial
640 community composition and C biogeochemistry of soils in a mesohaline marsh following
641 saltwater intrusion reported immediate changes in C mineralization rates with delayed shifts in
642 microbial community composition (Dang et al., 2019). Similarly, a 17-year dryland soil
643 transplant experiment showed large shifts in microbial activity with no change in community
644 composition (Bond-Lamberty et al., 2016). Furthermore, studies across diverse systems show
645 disconnect in function and composition. For example, C chemistry and not microbial community

646 structure or gene expression was found to significantly influence freshwater hyporheic zone
647 organic matter processing (Graham et al., 2018); environmental conditions influenced the
648 distribution of functional groups, but not taxonomic composition of marine bacterial and
649 archaeal communities (Lima-Mendez et al., 2015; Louca et al., 2016); and dynamic community
650 shifts did not impact functional stability of a methanogenic reactor (Fernández et al., 1999).
651 Combining our study with these previous investigations provides evidence that is consistent with
652 (but does not prove) that soil microbial community composition can be independent of C
653 chemistry, though this certainly varies across systems (e.g., Stegen et al. 2018).

654
655 In our system, lack of an association between microbial composition and organic C chemistry is
656 also likely due to a strong influence of stochastic community assembly. Our null modeling
657 indicated that dispersal limitation was responsible for 54% of variation in community
658 composition. Dispersal limitation influences composition by restricting the movement of
659 organisms through space. Restricted movement enhances the influences of stochastic ecological
660 drift, which arises through birth and death events that are randomly distributed across taxa
661 (Green et al., 2004, 2008; Hubbell, 2001; Martiny et al., 2006; McClain et al., 2012; Stegen et
662 al., 2015). Because ecological drift (enabled by dispersal limitation) can lead to the random loss
663 of taxa within local communities, it can result in different communities containing different, but
664 functionally redundant taxa (Loreau, 2004). Moreover, one can argue as per Louca et al., 2018
665 that in an open system with regular exposure to external inputs (e.g., via tides), functional
666 redundancy is expected to occur and lead to a decoupling of microbial structure and function
667 (Burke et al., 2011; Liebold and Chase, 2017; Nemergut et al., 2013b).

668

669 **Conclusions**

670 Our results have revealed landscape scale gradients in soil C chemistry in a coastal forested
671 floodplain, but also show that such gradients are different across soil depths and OC fractions—
672 occurring only in the shallow, water soluble C pool. In addition, we found little evidence of an
673 association between C chemistry and microbial community assembly processes, likely due to a
674 dominant influence of stochastic community assembly (as indicated by a strong influence of
675 dispersal limitation). We propose that the disconnect between C chemistry and microbial
676 communities is enhanced by differences in the time scales for which C chemistry and microbial
677 community composition shift.

678

679 Our findings suggest that cross-system heterogeneity observed in coastal soil biogeochemical
680 responses to salinity are likely associated with molecular-level C chemistry and microbial
681 physiological responses that are contingent on historical conditions (Fig. 6) (Goldman et al.,
682 2017; Hawkes and Keitt, 2015; Hawkes et al., 2017; Stegen et al., 2018a). We further suggest
683 that microbial community composition may not strongly influence biogeochemical function in
684 coastal soils. Processes associated with molecular-level C chemistry dynamics are therefore
685 likely to be a critical component of ecosystem responses to changing salinity dynamics in coastal
686 TAIs. A full elucidation of these processes will lay a foundation for the development of
687 mechanistic models of coastal TAI biogeochemical dynamics, providing an opportunity for
688 better representation of these ecosystems in local, regional, and Earth system models.

689

690 **Code and data availability**

691 Raw sequence data has been uploaded to the National Center for Biotechnology Information's
692 (NCBI) Sequence Read Archive (SRA) under BioProject PRJNA541992. All other data are
693 available at DataHub (a PNNL database server) upon manuscript acceptance. Original codes for

694 community assembly metric calculation are available at Stegen_etal_ISME 2013 github
695 repository https://github.com/stegen/Stegen_etal_ISME_2013.

696

697 **Author contribution**

698 AS designed the study, performed the experiments, conducted data analyses and interpretation,
699 and wrote the original draft. JI and CG collected the samples and created site maps. MTF, RKC,
700 and JT provided input on FTICR methodology, conducted the FTICR-MS instrument run, and
701 handled quality filtering and pre-processing of FTICR scans. VLB and NDW contributed to
702 funding acquisition, site selection, study design conceptualization, interpretation of results and
703 editing. JCS contributed to funding acquisition, study design conceptualization, interpretation of
704 results, reviewing and editing. All authors provided feedback on the manuscript.

705

706 **Competing interests**

707 The authors declare no conflict of interest.

708

709 **Acknowledgements**

710 This work is part of the PREMIS Initiative at Pacific Northwest National Laboratory (PNNL). It
711 was conducted under the Laboratory Directed Research and Development Program at PNNL, a
712 multi-program national laboratory operated by Battelle for the U.S. Department of Energy under
713 Contract DE-AC05-76RL01830. A portion of the research was performed using EMSL
714 (grid.436923.9), a DOE Office of Science User Facility sponsored by the Office of Biological

715 and Environmental Research. We would like to acknowledge Yuliya Farris and Sarah Fansler for
716 DNA extraction and sequencing respectively, Colin Brislawn for processing amplicon-sequence
717 data, and the Central Analytical Laboratory at Oregon State University for conducting soil
718 chemical analysis.

719

720 **References**

721 Ardón, M., Helton, A. M. and Bernhardt, E. S.: Drought and saltwater incursion synergistically
722 reduce dissolved organic carbon export from coastal freshwater wetlands, *Biogeochemistry*,
723 127(2–3), 411–426, doi:10.1007/s10533-016-0189-5, 2016.

724 Ardón, M., Helton, A. M. and Bernhardt, E. S.: Salinity effects on greenhouse gas emissions
725 from wetland soils are contingent upon hydrologic setting: a microcosm experiment,
726 *Biogeochemistry*, 140(2), 217–232, doi:10.1007/s10533-018-0486-2, 2018.

727 Aronesty, E. Comparison of sequencing utility programs. *The Open Bioinformatics Journal* 7, 1-
728 8 (2013).

729 Bailey, V. L., Smith, A. P., Tfaily, M., Fansler, S. J. and Bond-Lamberty, B.: Differences in
730 soluble organic carbon chemistry in pore waters sampled from different pore size domains, *Soil*
731 *Biol. Biochem.*, 107, 133–143, doi:10.1016/J.SOILBIO.2016.11.025, 2017.

732 Barry, S. C., Bianchi, T. S., Shields, M. R., Hutchings, J. A., Jacoby, C. A. and Frazer, T. K.:
733 Characterizing blue carbon stocks in *Thalassia testudinum* meadows subjected to different
734 phosphorus supplies: A lignin biomarker approach, *Limnol. Oceanogr.*, doi:10.1002/lno.10965,
735 2018.

736 BBMap: a fast, accurate, splice-aware aligner (2014).

737 Bischoff, N., Mikutta, R., Shibistova, O., Dohrmann, R., Herdtle, D., Gerhard, L., Fritzsche, F.,
738 Puzanov, A., Silanteva, M., Grebennikova, A. and Guggenberger, G.: Organic matter dynamics
739 along a salinity gradient in Siberian steppe soils, *Biogeosciences*, 15, 13–29, doi:10.5194/bg-15-
740 13-2018, 2018.

741 Bond-Lamberty, B., Bolton, H., Fansler, S., Heredia-Langner, A., Liu, C., McCue, L. A., Smith,
742 J. and Bailey, V.: Soil Respiration and Bacterial Structure and Function after 17 Years of a
743 Reciprocal Soil Transplant Experiment, edited by K. Treseder, *PLoS One*, 11(3), e0150599,
744 doi:10.1371/journal.pone.0150599, 2016.

745 Bottos, E. M., Kennedy, D. W., Romero, E. B., Fansler, S. J., Brown, J. M., Bramer, L. M., Chu,
746 R. K., Tfaily, M. M., Jansson, J. K. and Stegen, J. C.: Dispersal limitation and thermodynamic
747 constraints govern spatial structure of permafrost microbial communities, *FEMS Microbiol.*
748 *Ecol.*, 94(8), doi:10.1093/femsec/fiy110, 2018.

749 Boye, K., Noël, V., Tfaily, M. M., Bone, S. E., Williams, K. H., Bargar, J. R. and Fendorf, S.:

750 Thermodynamically controlled preservation of organic carbon in floodplains, ,
751 doi:10.1038/NGEO2940, 2017.

752 Bramucci, A., Han, S., Beckers, J., Haas, C., Lanoil, B., Bramucci, A., Han, S., Beckers, J.,
753 Haas, C. and Lanoil, B.: Composition, Diversity, and Stability of Microbial Assemblages in
754 Seasonal Lake Ice, Miquelon Lake, Central Alberta, *Biology (Basel)*, 2(2), 514–532,
755 doi:10.3390/biology2020514, 2013.

756 Breitling, R., Ritchie, S., Goodenowe, D., Stewart, M. L. and Barrett, M. P.: Ab initio prediction
757 of metabolic networks using Fourier transform mass spectrometry data, *Metabolomics*, 2(3),
758 155–164, doi:10.1007/s11306-006-0029-z, 2006.

759 Brown, J., Zavoshy, N., Brislawn, C. J. and McCue, L. A.: Hundo: a Snakemake workflow for
760 microbial community sequence data, , doi:10.7287/peerj.preprints.27272v1, 2018.

761 Burke, C., Steinberg, P., Rusch, D., Kjelleberg, S. and Thomas, T.: Bacterial community
762 assembly based on functional genes rather than species., *Proc. Natl. Acad. Sci. U. S. A.*, 108(34),
763 14288–93, doi:10.1073/pnas.1101591108, 2011.

764 Caruso, T., Chan, Y., Lacap, D. C., Lau, M. C. Y., McKay, C. P. and Pointing, S. B.: Stochastic
765 and deterministic processes interact in the assembly of desert microbial communities on a global
766 scale., *ISME J.*, 5(9), 1406–13, doi:10.1038/ismej.2011.21, 2011.

767 Chambers, L. G., Reddy, K. R. and Osborne, T. Z.: Short-Term Response of Carbon Cycling to
768 Salinity Pulses in a Freshwater Wetland, *Soil Sci. Soc. Am. J.*, 75(5), 2000,
769 doi:10.2136/sssaj2011.0026, 2011.

770 Chambers, L. G., Osborne, T. Z. and Reddy, K. R.: Effect of salinity-altering pulsing events on
771 soil organic carbon loss along an intertidal wetland gradient: a laboratory experiment,
772 *Biogeochemistry*, 115(1–3), 363–383, doi:10.1007/s10533-013-9841-5, 2013.

773 Chambers, L. G., Davis, S. E., Troxler, T., Boyer, J. N., Downey-Wall, A. and Scinto, L. J.:
774 Biogeochemical effects of simulated sea level rise on carbon loss in an Everglades mangrove
775 peat soil, *Hydrobiologia*, 726(1), 195–211, doi:10.1007/s10750-013-1764-6, 2014.

776 Conant, R. T., Ogle, S. M., Paul, E. A. and Paustian, K.: Measuring and monitoring soil organic
777 carbon stocks in agricultural lands for climate mitigation, *Front. Ecol. Environ.*, 9(3), 169–173,
778 doi:10.1890/090153, 2011.

779 Conrads, P. A. and Darby, L. S.: Development of a coastal drought index using salinity data,
780 *Bull. Am. Meteorol. Soc.*, 98(4), 753–766, doi:10.1175/BAMS-D-15-00171.1, 2017.

781 Dang, C., Morrissey, E. M., Neubauer, S. C. and Franklin, R. B.: Novel microbial community
782 composition and carbon biogeochemistry emerge over time following saltwater intrusion in
783 wetlands, *Glob. Chang. Biol.*, (September 2018), 549–561, doi:10.1111/gcb.14486, 2019.

784 Dini-Andreote, F., Stegen, J. C., van Elsas, J. D. and Salles, J. F.: Disentangling mechanisms that
785 mediate the balance between stochastic and deterministic processes in microbial succession.,
786 *Proc. Natl. Acad. Sci. U. S. A.*, 112(11), E1326-32, doi:10.1073/pnas.1414261112, 2015.

787 Dittmar, T., Koch, B., Hertkorn, N. and Kattner, G.: A simple and efficient method for the solid-
788 phase extraction of dissolved organic matter (SPE-DOM) from seawater, *Limnol. Ocean.*,
789 *Methods* 6, 230–235 [online] Available from:

790 <https://aslopubs.onlinelibrary.wiley.com/doi/pdf/10.4319/lom.2008.6.230> (Accessed 16 April
791 2019a), 2008.

792 Dittmar, T., Koch, B., Hertkorn, N. and Kattner, G.: A simple and efficient method for the solid-
793 phase extraction of dissolved organic matter (SPE-DOM) from seawater, *Epic. Oceanogr.*
794 *Methods*, 6, pp. 230-235, 2008b.

795 Dungait, J. A. J., Hopkins, D. W., Gregory, A. S. and Whitmore, A. P.: Soil organic matter
796 turnover is governed by accessibility not recalcitrance, *Glob. Chang. Biol.*, 18(6), 1781–1796,
797 doi:10.1111/j.1365-2486.2012.02665.x, 2012.

798 Edgar, R. C. Search and clustering orders of magnitude faster than BLAST. *Bioinformatics*
799 **26**, 2460-2461 (2010).

800

801 Ensign, S. H. and Noe, G. B.: Tidal extension and sea-level rise: recommendations for a research
802 agenda, *Front. Ecol. Environ.*, 16(1), 37–43, doi:10.1002/fee.1745, 2018.

803 Fernández, A., Huang, S., Seston, S., Xing, J., Hickey, R., Criddle, C. and Tiedje, J.: How stable
804 is stable? Function versus community composition., *Appl. Environ. Microbiol.*, 65(8), 3697–704
805 [online] Available from: <http://www.ncbi.nlm.nih.gov/pubmed/10427068> (Accessed 27 March
806 2019), 1999.

807 Fierer, N.: Embracing the unknown: disentangling the complexities of the soil microbiome, *Nat.*
808 *Publ. Gr.*, doi:10.1038/nrmicro.2017.87, 2017.

809 Fierer, N. and Jackson, R. B.: The diversity and biogeography of soil bacterial communities.
810 [online] Available from: www.pnas.org/cgi/doi/10.1073/pnas.0507535103 (Accessed 8 February
811 2019), 2006.

812 Garbeva, P., van Veen, J. a and van Elsas, J. D.: Microbial diversity in soil: selection microbial
813 populations by plant and soil type and implications for disease suppressiveness., *Annu. Rev.*
814 *Phytopathol.*, 42(29), 243–70, doi:10.1146/annurev.phyto.42.012604.135455, 2004.

815 Goldman, A. E., Graham, E. B., Crump, A. R., Kennedy, D. W., Romero, E. B., Anderson, C.
816 G., Dana, K. L., Resch, C. T., Fredrickson, J. K. and Stegen, J. C.: Biogeochemical cycling at the
817 aquatic–terrestrial interface is linked to parafluvial hyporheic zone inundation history,
818 *Biogeosciences*, 14(18), 4229–4241, doi:10.5194/bg-14-4229-2017, 2017.

819 Gouffi, K., Pica, N., Pichereau, V. and Blanco, C.: Disaccharides as a new class of
820 nonaccumulated osmoprotectants for *Sinorhizobium meliloti*., *Appl. Environ. Microbiol.*, 65(4),
821 1491–500 [online] Available from: <http://www.ncbi.nlm.nih.gov/pubmed/10103242> (Accessed 8
822 October 2018a), 1999.

823 Gouffi, K., Pica, N., Pichereau, V. and Blanco, C.: Disaccharides as a new class of
824 nonaccumulated osmoprotectants for *Sinorhizobium meliloti*, *Appl. Environ. Microbiol.*, 65(4),
825 1491–1500, doi:10.1186/1746-1448-1-5, 1999b.

826 Graham, E. B., Knelman, J. E., Schindlbacher, A., Siciliano, S., Breulmann, M., Yannarell, A.,
827 Beman, J. M., Abell, G., Philippot, L., Prosser, J., Foulquier, A., Yuste, J. C., Glanville, H. C.,
828 Jones, D. L., Angel, R., Salminen, J., Newton, R. J., Bürgmann, H., Ingram, L. J., Hamer, U.,
829 Siljanen, H. M. P., Peltoniemi, K., Potthast, K., Bañeras, L., Hartmann, M., Banerjee, S., Yu, R.-
830 Q., Nogaro, G., Richter, A., Koranda, M., Castle, S. C., Goberna, M., Song, B., Chatterjee, A.,

831 Nunes, O. C., Lopes, A. R., Cao, Y., Kaisermann, A., Hallin, S., Strickland, M. S., Garcia-
832 Pausas, J., Barba, J., Kang, H., Isobe, K., Papaspyrou, S., Pastorelli, R., Lagomarsino, A.,
833 Lindström, E. S., Basiliko, N. and Nemergut, D. R.: Microbes as Engines of Ecosystem
834 Function: When Does Community Structure Enhance Predictions of Ecosystem Processes?,
835 *Front. Microbiol.*, 7, 214, doi:10.3389/fmicb.2016.00214, 2016.

836 Graham, E. B., Tfaily, M. M., Crump, A. R., Goldman, A. E., Bramer, L. M., Arntzen, E.,
837 Romero, E., Resch, C. T., Kennedy, D. W. and Stegen, J. C.: Carbon Inputs From Riparian
838 Vegetation Limit Oxidation of Physically Bound Organic Carbon Via Biochemical and
839 Thermodynamic Processes, *J. Geophys. Res. Biogeosciences*, 122(12), 3188–3205,
840 doi:10.1002/2017JG003967, 2017a.

841 Graham, E. B., Crump, A. R., Resch, C. T., Fansler, S., Arntzen, E., Kennedy, D. W.,
842 Fredrickson, J. K. and Stegen, J. C.: Deterministic influences exceed dispersal effects on
843 hydrologically-connected microbiomes, *Environ. Microbiol.*, 19(4), 1552–1567,
844 doi:10.1111/1462-2920.13720, 2017b.

845 Graham, E. B., Crump, A. R., Kennedy, D. W., Arntzen, E., Fansler, S., Purvine, S. O., Nicora,
846 C. D., Nelson, W., Tfaily, M. M. and Stegen, J. C.: Multi 'omics comparison reveals
847 metabolome biochemistry, not microbiome composition or gene expression, corresponds to
848 elevated biogeochemical function in the hyporheic zone, *Sci. Total Environ.*, 642, 742–753,
849 doi:10.1016/J.SCITOTENV.2018.05.256, 2018.

850 Green, J. L., Holmes, A. J., Westoby, M., Oliver, I., Briscoe, D., Dangerfield, M., Gillings, M.
851 and Beattie, A. J.: Spatial scaling of microbial eukaryote diversity, *Nature*, 432(7018), 747–750,
852 doi:10.1038/nature03034, 2004.

853 Green, J. L., Bohannan, B. J. M. and Whitaker, R. J.: Microbial Biogeography: From Taxonomy
854 to Traits, *Science (80-.)*, 320(5879), 1039–1043, doi:10.1126/SCIENCE.1153475, 2008.

855 Guillemette, R., Kaneko, R., Blanton, J., Tan, J., Witt, M., Hamilton, S., Allen, E. E., Medina,
856 M., Hamasaki, K., Koch, B. P. and Azam, F.: Bacterioplankton drawdown of coral mass-
857 spawned organic matter, *ISME J.*, 12(9), 2238–2251, doi:10.1038/s41396-018-0197-7, 2018.

858 Hawkes, C. V. and Keitt, T. H.: Resilience vs. historical contingency in microbial responses to
859 environmental change, edited by A. Classen, *Ecol. Lett.*, 18(7), 612–625, doi:10.1111/ele.12451,
860 2015.

861 Hawkes, C. V., Waring, B. G., Rocca, J. D. and Kivlin, S. N.: Historical climate controls soil
862 respiration responses to current soil moisture., *Proc. Natl. Acad. Sci. U. S. A.*, 114(24), 6322–
863 6327, doi:10.1073/pnas.1620811114, 2017.

864 Hedges, J. I. and Oades, J. M.: Comparative organic geochemistries of soils and marine
865 sediments, *Org. Geochem*, 27(7/8), 319–361 [online] Available from:
866 http://www.riversystems.washington.edu/lc/RIVERS/93_hedges_ji_27-319-361.pdf (Accessed 7
867 May 2019), 1997.

868 Hedges, J. I., Keil, R. G. and Benner, R.: What happens to terrestrial organic matter in the
869 ocean?, *Org. Geochem.*, 27(5–6), 195–212, doi:10.1016/S0146-6380(97)00066-1, 1997.

870 Herbert, E. R., Schubauer-Berigan, J. and Craft, C. B.: Differential effects of chronic and acute
871 simulated seawater intrusion on tidal freshwater marsh carbon cycling, *Biogeochemistry*, 138(2),

872 137–154, doi:10.1007/s10533-018-0436-z, 2018.

873 Hinson, A. L., Feagin, R. A., Eriksson, M., Najjar, R. G., Herrmann, M., Bianchi, T. S., Kemp,
874 M., Hutchings, J. A., Crooks, S. and Boutton, T.: The spatial distribution of soil organic carbon
875 in tidal wetland soils of the continental United States, *Glob. Chang. Biol.*, 23(12), 5468–5480,
876 doi:10.1111/gcb.13811, 2017.

877 Hoitink, A. J. F. and Jay, D. A.: Tidal river dynamics: Implications for deltas, *Rev. Geophys.*,
878 54(1), 240–272, doi:10.1002/2015RG000507, 2016.

879 Hoitink, A. J. F., Buschman, F. A. and Vermeulen, B.: Continuous measurements of discharge
880 from a horizontal acoustic Doppler current profiler in a tidal river, *Water Resour. Res.*, 45, 11406,
881 doi:10.1029/2009WR007791, 2009.

882 Holmquist, J. R., Windham-Myers, L., Bliss, N., Crooks, S., Morris, J. T., Megonigal, J. P.,
883 Troxler, T., Weller, D., Callaway, J., Drexler, J., Ferner, M. C., Gonnee, M. E., Kroeger, K. D.,
884 Schile-Beers, L., Woo, I., Buffington, K., Breithaupt, J., Boyd, B. M., Brown, L. N., Dix, N.,
885 Hice, L., Horton, B. P., MacDonald, G. M., Moyer, R. P., Reay, W., Shaw, T., Smith, E., Smoak,
886 J. M., Sommerfield, C., Thorne, K., Velinsky, D., Watson, E., Grimes, K. W. and Woodrey, M.:
887 Accuracy and Precision of Tidal Wetland Soil Carbon Mapping in the Conterminous United
888 States, *Sci. Rep.*, 8(1), 9478, doi:10.1038/s41598-018-26948-7, 2018.

889 Hubbell, S. P.: *The Unified Neutral Theory of Biodiversity and Biogeography*, Princeton
890 University Press. [online] Available from: <http://www.jstor.org/stable/j.ctt7rj8w>, 2001.

891 Jobbágy, E. G. and Jackson, R. B.: The vertical distribution of soil organic carbon and its relation
892 to climate and vegetation, *Ecol. Appl.*, 10(2), 423–436, doi:10.1890/1051-
893 0761(2000)010[0423:TVDOSO]2.0.CO;2, 2000.

894 Kim, S., Kramer, R. W. and Hatcher, P. G.: Graphical Method for Analysis of Ultrahigh-
895 Resolution Broadband Mass Spectra of Natural Organic Matter, the Van Krevelen Diagram,
896 *Anal. Chem.*, 75(20), 5336–5344, doi:10.1021/ac034415p, 2003.

897 Koch, B. P. and Dittmar, T.: From mass to structure: an aromaticity index for high-resolution
898 mass data of natural organic matter, *Rapid Commun. Mass Spectrom.*, 20(5), 926–932,
899 doi:10.1002/rcm.2386, 2006.

900 Koch, B. P. and Dittmar, T.: From mass to structure: an aromaticity index for high-resolution
901 mass data of natural organic matter, *Rapid Commun. Mass Spectrom.*, 30(1), 250–250,
902 doi:10.1002/rcm.7433, 2016.

903 Koch, B. P., Kattner, G., Witt, M. and Passow, U.: Molecular insights into the microbial
904 formation of marine dissolved organic matter: recalcitrant or labile?, *Biogeosciences*, 11(15),
905 4173–4190, doi:10.5194/bg-11-4173-2014, 2014.

906 Kramer, C. and Gleixner, G.: Variable use of plant- and soil-derived carbon by microorganisms
907 in agricultural soils, *Soil Biol. Biochem.*, 38(11), 3267–3278,
908 doi:10.1016/J.SOILBIO.2006.04.006, 2006.

909 Kramer, C. and Gleixner, G.: Soil organic matter in soil depth profiles: Distinct carbon
910 preferences of microbial groups during carbon transformation, *Soil Biol. Biochem.*, 40(2), 425–
911 433, doi:10.1016/J.SOILBIO.2007.09.016, 2008.

912 Krauss, K. W., Noe, G. B., Duberstein, J. A., Conner, W. H., Stagg, C. L., Cormier, N., Jones,
913 M. C., Bernhardt, C. E., Graeme Lockaby, B., From, A. S., Doyle, T. W., Day, R. H., Ensign, S.
914 H., Pierfelice, K. N., Hupp, C. R., Chow, A. T. and Whitbeck, J. L.: The Role of the Upper Tidal
915 Estuary in Wetland Blue Carbon Storage and Flux, *Global Biogeochem. Cycles*, 32(5), 817–839,
916 doi:10.1029/2018GB005897, 2018.

917 Ksionzek, K. B., Lechtenfeld, O. J., McCallister, S. L., Schmitt-Kopplin, P., Geuer, J. K.,
918 Geibert, W. and Koch, B. P.: Dissolved organic sulfur in the ocean: Biogeochemistry of a
919 petagram inventory., *Science*, 354(6311), 456–459, doi:10.1126/science.aaf7796, 2016.

920 Kubartová, A., Ottosson, E. and Stenlid, J.: Linking fungal communities to wood density loss
921 after 12 years of log decay, *FEMS Microbiol. Ecol.*, 91(5), doi:10.1093/femsec/fiv032, 2015.

922 Kujawinski, E. B. and Behn, M. D.: Automated analysis of electrospray ionization fourier
923 transform ion cyclotron resonance mass spectra of natural organic matter., *Anal. Chem.*, 78(13),
924 4363–73, doi:10.1021/ac0600306, 2006.

925 Langer, U. and Rinklebe, J.: Lipid biomarkers for assessment of microbial communities in
926 floodplain soils of the Elbe River (Germany), *Wetlands*, 29(1), 353–362, doi:10.1672/08-114.1,
927 2009.

928 Langley, J. A., Sigrist, M. V, Duls, J., Cahoon, D. R., Lynch, J. C. and Megonigal, J. P.: Global
929 Change and Marsh Elevation Dynamics: Experimenting Where Land Meets Sea and Biology
930 Meets Geology, in *Proceedings of the Smithsonian Marine Sciences Symposium*, pp. 391–400,
931 Smithsonian Institution Scholarly Press, , Washington, DC. [online] Available from:
932 [https://repository.si.edu/bitstream/handle/10088/18988/serc_Langley_et_al._2009_Smithsonian_](https://repository.si.edu/bitstream/handle/10088/18988/serc_Langley_et_al._2009_Smithsonian_Marine_Sciences_.pdf?sequence=1&isAllowed=y)
933 [Marine_Sciences_.pdf?sequence=1&isAllowed=y](https://repository.si.edu/bitstream/handle/10088/18988/serc_Langley_et_al._2009_Smithsonian_Marine_Sciences_.pdf?sequence=1&isAllowed=y) (Accessed 7 May 2019), 2007.

934 Langston, A. K., Kaplan, D. A. and Putz, F. E.: A casualty of climate change? Loss of freshwater
935 forest islands on Florida’s Gulf Coast, *Glob. Chang. Biol.*, 23(12), 5383–5397,
936 doi:10.1111/gcb.13805, 2017.

937 LaRowe, D. E. and Van Cappellen, P.: Degradation of natural organic matter: A thermodynamic
938 analysis, *Geochim. Cosmochim. Acta*, 75(8), 2030–2042, doi:10.1016/J.GCA.2011.01.020,
939 2011.

940 Lechtenfeld, O. J., Hertkorn, N., Shen, Y., Witt, M. and Benner, R.: Marine sequestration of
941 carbon in bacterial metabolites., *Nat. Commun.*, 6(1), 6711, doi:10.1038/ncomms7711, 2015.

942 Liebold, M. A. and Chase, M. J.: Combining Taxonomic and Functional Patterns to Disentangle
943 Metacommunity Assembly Processes, in *Metacommunity Ecology*, Volume 9, edited by M. A.
944 Liebold and M. J. Chase, p. 504, Princeton University Press, Princeton, New Jersey., 2017.

945 Lima-Mendez, G., Faust, K., Henry, N., Decelle, J., Colin, S., Carcillo, F., Chaffron, S., Ignacio-
946 Espinosa, J. C., Roux, S., Vincent, F., Bittner, L., Darzi, Y., Wang, J., Audic, S., Berline, L.,
947 Bontempi, G., Cabello, A. M., Coppola, L., Cornejo-Castillo, F. M., d’Ovidio, F., Meester, L.
948 De, Ferrera, I., Garet-Delmas, M.-J., Guidi, L., Lara, E., Pesant, S., Royo-Llonch, M., Salazar,
949 G., Sánchez, P., Sebastian, M., Souffreau, C., Dimier, C., Picheral, M., Searson, S., Kandels-
950 Lewis, S., coordinators, T. O., Gorsky, G., Not, F., Ogata, H., Speich, S., Stemmann, L.,
951 Weissenbach, J., Wincker, P., Acinas, S. G., Sunagawa, S., Bork, P., Sullivan, M. B., Karsenti,
952 E., Bowler, C., Vargas, C. de and Raes, J.: Determinants of community structure in the global

953 plankton interactome, *Science* (80-.), 348(6237), 1262073, doi:10.1126/SCIENCE.1262073,
954 2015.

955 Liu, X., Ruecker, A., Song, B., Xing, J., Conner, W. H. and Chow, A. T.: Effects of salinity and
956 wet–dry treatments on C and N dynamics in coastal-forested wetland soils: Implications of sea
957 level rise, *Soil Biol. Biochem.*, 112, 56–67, doi:10.1016/J.SOILBIO.2017.04.002, 2017.

958 Loreau, M.: Does functional redundancy exist?, *Oikos*, 104(3), 606–611, doi:10.1111/j.0030-
959 1299.2004.12685.x, 2004.

960 Louca, S., Parfrey, L. W. and Doebeli, M.: Decoupling function and taxonomy in the global
961 ocean microbiome., *Science*, 353(6305), 1272–7, doi:10.1126/science.aaf4507, 2016.

962 Louca, S., Polz, M. F., Mazel, F., Albright, M. B. N., Huber, J. A., O’connor, M. I., Ackermann,
963 M., Hahn, A. S., Srivastava, D. S., Crowe, S. A., Doebeli, M. and Parfrey, L. W.: Disentangling
964 function from taxonomy in microbial systems Function and functional redundancy in microbial
965 systems, , doi:10.1038/s41559-018-0519-1, 2018.

966 Martiny, J. B. H., Bohannan, B. J. M., Brown, J. H., Colwell, R. K., Fuhrman, J. A., Green, J. L.,
967 Horner-Devine, M. C., Kane, M., Krumins, J. A., Kuske, C. R., Morin, P. J., Naeem, S., Øvreås,
968 L., Reysenbach, A.-L., Smith, V. H. and Staley, J. T.: Microbial biogeography: putting
969 microorganisms on the map, *Nat. Rev. Microbiol.*, 4(2), 102–112, doi:10.1038/nrmicro1341,
970 2006.

971 Marton, J. M., Herbert, E. R. and Craft, C. B.: Effects of Salinity on Denitrification and
972 Greenhouse Gas Production from Laboratory-incubated Tidal Forest Soils, *Wetlands*, 32(2),
973 347–357, doi:10.1007/s13157-012-0270-3, 2012.

974 Mau, R. L., Liu, C. M., Aziz, M., Schwartz, E., Dijkstra, P., Marks, J. C., Price, L. B., Keim, P.
975 and Hungate, B. A.: Linking soil bacterial biodiversity and soil carbon stability, *ISME J.*, 9(6),
976 1477–1480, doi:10.1038/ismej.2014.205, 2015.

977 McCarthy, M., Dimmitt, B., Muller-Karger, F., McCarthy, M. J., Dimmitt, B. and Muller-
978 Karger, F. E.: Rapid Coastal Forest Decline in Florida’s Big Bend, *Remote Sens.*, 10(11), 1721,
979 doi:10.3390/rs10111721, 2018.

980 McClain, C. R., Stegen, J. C. and Hurlbert, A. H.: Dispersal, environmental niches and oceanic-
981 scale turnover in deep-sea bivalves, *Proc. R. Soc. B Biol. Sci.*, doi:10.1098/RSPB.2011.2166,
982 2012.

983 Medeiros, P. M., Seidel, M., Ward, N. D., Carpenter, E. J., Gomes, H. R., Niggemann, J.,
984 Krusche, A. V., Richey, J. E., Yager, P. L. and Dittmar, T.: Fate of the Amazon River dissolved
985 organic matter in the tropical Atlantic Ocean, *Global Biogeochem. Cycles*, 29(5), 677–690,
986 doi:10.1002/2015GB005115, 2015.

987 Minor, E. C., Steinbring, C. J., Longnecker, K. and Kujawinski, E. B.: Characterization of
988 dissolved organic matter in Lake Superior and its watershed using ultrahigh resolution mass
989 spectrometry, *Org. Geochem.*, 43, 1–11, doi:10.1016/J.ORGGEOCHEM.2011.11.007, 2012.

990 Nemergut, D. R., Schmidt, S. K., Fukami, T., O’Neill, S. P., Bilinski, T. M., Stanish, L. F.,
991 Knelman, J. E., Darcy, J. L., Lynch, R. C., Wickey, P. and Ferrenberg, S.: Patterns and processes
992 of microbial community assembly., *Microbiol. Mol. Biol. Rev.*, 77(3), 342–56,

- 993 doi:10.1128/MMBR.00051-12, 2013a.
- 994 Nemergut, D. R., Schmidt, S. K., Fukami, T., O'Neill, S. P., Bilinski, T. M., Stanish, L. F.,
995 Knelman, J. E., Darcy, J. L., Lynch, R. C., Wickey, P. and Ferrenberg, S.: Patterns and processes
996 of microbial community assembly., *Microbiol. Mol. Biol. Rev.*, 77(3), 342–56,
997 doi:10.1128/MMBR.00051-12, 2013b.
- 998 Neubauer, S. C., Givler, K., Valentine, S. and Megonigal, J. P.: Seasonal patterns and plant-
999 mediated controls of subsurface wetland biogeochemistry, *Ecology*, 86(12), 3334–3344,
1000 doi:10.1890/04-1951, 2005.
- 1001 Neubauer, S. C., Franklin, R. B. and Berrier, D. J.: Saltwater intrusion into tidal freshwater
1002 marshes alters the biogeochemical processing of organic carbon, *Biogeosciences*, 10(12), 8171–
1003 8183, doi:10.5194/bg-10-8171-2013, 2013a.
- 1004 Neubauer, S. C., Franklin, R. B. and Berrier, D. J.: Saltwater intrusion into tidal freshwater
1005 marshes alters the biogeochemical processing of organic carbon, *Biogeosciences*, 10(12), 8171–
1006 8183, doi:10.5194/bg-10-8171-2013, 2013b.
- 1007 Nyman, J. A. and Delaune, R. D.: CO₂ emission and soil Eh responses to different hydrological
1008 conditions in fresh, brackish, and saline marsh soils. [online] Available from:
1009 <https://aslopubs.onlinelibrary.wiley.com/doi/pdf/10.4319/lo.1991.36.7.1406> (Accessed 31
1010 October 2018), 1991.
- 1011 R Development Core Team: The R Project for Statistical Computing, [online] Available from:
1012 <https://www.r-project.org/> (Accessed 9 May 2019), 2019.
- 1013 Reynolds, L. L., Lajtha, K., Bowden, R. D., Tfaily, M. M., Johnson, B. R. and Bridgman, S. D.:
1014 The Path From Litter to Soil: Insights Into Soil C Cycling From Long-Term Input Manipulation
1015 and High-Resolution Mass Spectrometry, *J. Geophys. Res. Biogeosciences*, 123(5), 1486–1497,
1016 doi:10.1002/2017JG004076, 2018.
- 1017 Rivas-Ubach, A., Liu, Y., Bianchi, T. S., Tolić, N., Jansson, C. and Paša-Tolić, L.: Moving
1018 beyond the van Krevelen Diagram: A New Stoichiometric Approach for Compound
1019 Classification in Organisms, *Anal. Chem.*, 90(10), 6152–6160,
1020 doi:10.1021/acs.analchem.8b00529, 2018.
- 1021 Rocca, J. D., Hall, E. K., Lennon, J. T., Evans, S. E., Waldrop, M. P., Cotner, J. B., Nemergut,
1022 D. R., Graham, E. B. and Wallenstein, M. D.: Relationships between protein-encoding gene
1023 abundance and corresponding process are commonly assumed yet rarely observed, *ISME J.*, 9(8),
1024 1693–1699, doi:10.1038/ismej.2014.252, 2015.
- 1025 Sawakuchi, H. O., Neu, V., Ward, N. D., Barros, M. de L. C., Valerio, A. M., Gagne-Maynard,
1026 W., Cunha, A. C., Less, D. F. S., Diniz, J. E. M., Brito, D. C., Krusche, A. V. and Richey, J. E.:
1027 Carbon Dioxide Emissions along the Lower Amazon River, *Front. Mar. Sci.*, 4,
1028 doi:10.3389/fmars.2017.00076, 2017.
- 1029 Schmidt, M. W. I., Torn, M. S., Abiven, S., Dittmar, T., Guggenberger, G., Janssens, I. A.,
1030 Kleber, M., Kögel-Knabner, I., Lehmann, J., Manning, D. A. C., Nannipieri, P., Rasse, D. P.,
1031 Weiner, S. and Trumbore, S. E.: Persistence of soil organic matter as an ecosystem property,
1032 *Nature*, 478(7367), 49–56, doi:10.1038/nature10386, 2011.

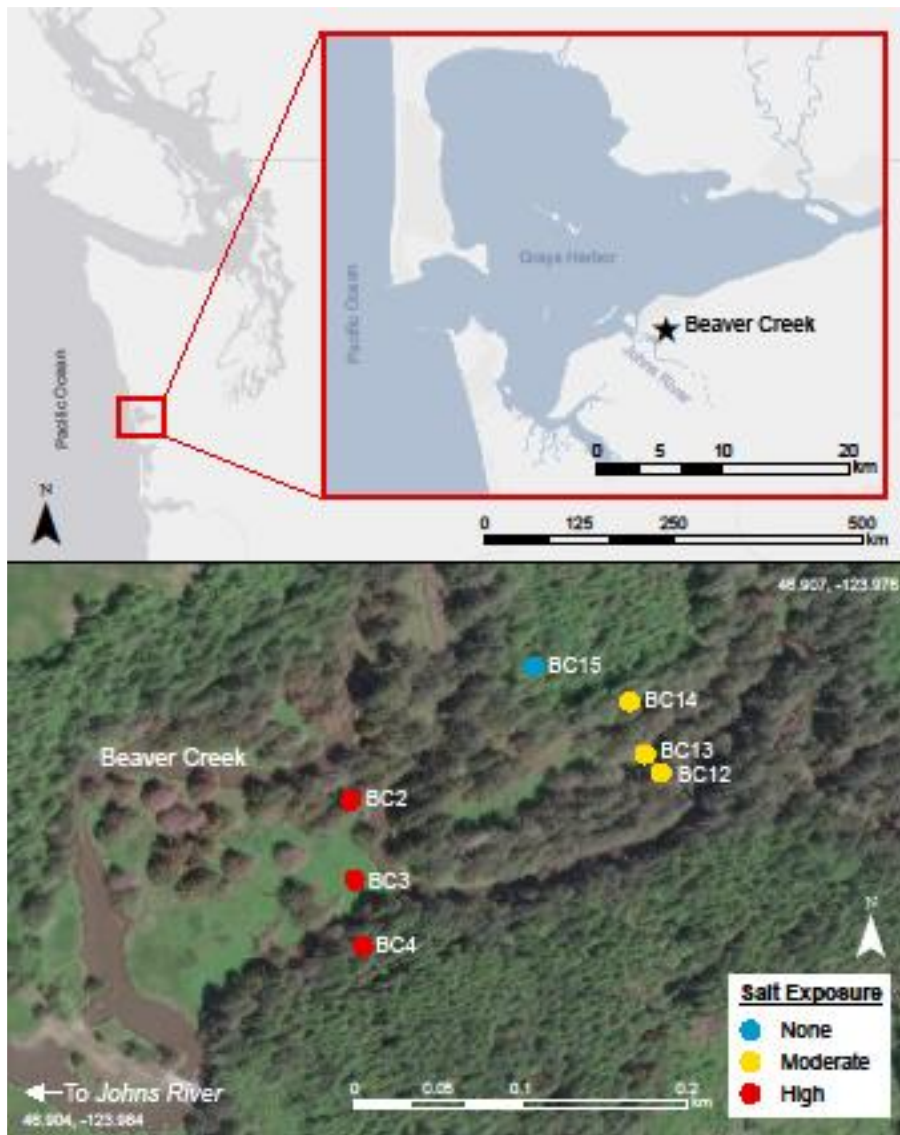
- 1033 Seidel, M., Dittmar, T., Ward, N. D., Krusche, A. V., Richey, J. E., Yager, P. L. and Medeiros,
1034 P. M.: Seasonal and spatial variability of dissolved organic matter composition in the lower
1035 Amazon River, *Biogeochemistry*, 131(3), 281–302, doi:10.1007/s10533-016-0279-4, 2016.
- 1036 Sengupta, A., Stegen, J. C., Meira Neto, A. A., Wang, Y., Neilson, J. W., Chorover, J., Troch, P.
1037 A., Maier, R. M., Chorover, J., Troch, P. A. and Maier, R. M.: Assessing Microbial Community
1038 Patterns During Incipient Soil Formation From Basalt, *J. Geophys. Res. Biogeosciences*, 124(4),
1039 941–958, doi:10.1029/2017JG004315, 2019.
- 1040 Shen, Y., Chapelle, F. H., Strom, E. W. and Benner, R.: Origins and bioavailability of dissolved
1041 organic matter in groundwater, *Biogeochemistry*, 122(1), 61–78, doi:10.1007/s10533-014-0029-
1042 4, 2015.
- 1043 Simon, C., Roth, V.-N., Dittmar, T. and Gleixner, G.: Molecular Signals of Heterogeneous
1044 Terrestrial Environments Identified in Dissolved Organic Matter: A Comparative Analysis of
1045 Orbitrap and Ion Cyclotron Resonance Mass Spectrometers, *Front. Earth Sci.*, 6, 138,
1046 doi:10.3389/feart.2018.00138, 2018.
- 1047 Sleator, R. D. and Hill, C.: Bacterial osmoadaptation: The role of osmolytes in bacterial stress
1048 and virulence, *FEMS Microbiol. Rev.*, 26(1), 49–71, doi:10.1016/S0168-6445(01)00071-7,
1049 2002.
- 1050 Smith, C. J., DeLaune, R. D. and Patrick, W. H.: Carbon dioxide emission and carbon
1051 accumulation in coastal wetlands, *Estuar. Coast. Shelf Sci.*, 17(1), 21–29, doi:10.1016/0272-
1052 7714(83)90042-2, 1983.
- 1053 Stegen, J. C., Lin, X., Konopka, A. E. and Fredrickson, J. K.: Stochastic and deterministic
1054 assembly processes in subsurface microbial communities., *ISME J.*, 6(9), 1653–64,
1055 doi:10.1038/ismej.2012.22, 2012.
- 1056 Stegen, J. C., Lin, X., Fredrickson, J. K., Chen, X., Kennedy, D. W., Murray, C. J., Rockhold, M.
1057 L. and Konopka, A.: Quantifying community assembly processes and identifying features that
1058 impose them, *ISME J.*, 7(11), 2069–2079, doi:10.1038/ismej.2013.93, 2013.
- 1059 Stegen, J. C., Lin, X., Fredrickson, J. K. and Konopka, A. E.: Estimating and mapping ecological
1060 processes influencing microbial community assembly, *Front. Microbiol.*, 6, 370,
1061 doi:10.3389/fmicb.2015.00370, 2015.
- 1062 Stegen, J. C., Bottos, E. M. and Jansson, J. K.: A unified conceptual framework for prediction
1063 and control of microbiomes, *Curr. Opin. Microbiol.*, 44, 20–27, doi:10.1016/J.MIB.2018.06.002,
1064 2018a.
- 1065 Stegen, J. C., Johnson, T., Fredrickson, J. K., Wilkins, M. J., Konopka, A. E., Nelson, W. C.,
1066 Arntzen, E. V., Chrisler, W. B., Chu, R. K., Fansler, S. J., Graham, E. B., Kennedy, D. W.,
1067 Resch, C. T., Tfaily, M. and Zachara, J.: Influences of organic carbon speciation on hyporheic
1068 corridor biogeochemistry and microbial ecology, *Nat. Commun.*, 9(1), 1–11,
1069 doi:10.1038/s41467-018-02922-9, 2018b.
- 1070 Stegen, J. C., Johnson, T., Fredrickson, J. K., Wilkins, M. J., Konopka, A. E., Nelson, W. C.,
1071 Arntzen, E. V., Chrisler, W. B., Chu, R. K., Fansler, S. J., Graham, E. B., Kennedy, D. W.,
1072 Resch, C. T., Tfaily, M. and Zachara, J.: Influences of organic carbon speciation on hyporheic
1073 corridor biogeochemistry and microbial ecology, *Nat. Commun.*, 9(1), 585, doi:10.1038/s41467-

- 1074 018-02922-9, 2018c.
- 1075 Steinmuller, H. E. and Chambers, L. G.: Can Saltwater Intrusion Accelerate Nutrient Export
1076 from Freshwater Wetland Soils? An Experimental Approach, *Soil Sci. Soc. Am. J.*, 82(1), 283,
1077 doi:10.2136/sssaj2017.05.0162, 2018.
- 1078 Tank, S. E., Fellman, J. B., Hood, E. and Kritzberg, E. S.: Beyond respiration: Controls on lateral
1079 carbon fluxes across the terrestrial-aquatic interface, *Limnol. Oceanogr. Lett.*, 3(3), 76–88,
1080 doi:10.1002/lol2.10065, 2018.
- 1081 Tfaily, M. M., Hodgkins, S., Podgorski, D. C., Chanton, J. P. and Cooper, W. T.: Comparison of
1082 dialysis and solid-phase extraction for isolation and concentration of dissolved organic matter
1083 prior to Fourier transform ion cyclotron resonance mass spectrometry, *Anal. Bioanal. Chem.*,
1084 404(2), 447–457, doi:10.1007/s00216-012-6120-6, 2012.
- 1085 Tfaily, M. M., Cooper, W. T., Kostka, J. E., Chanton, P. R., Schadt, C. W., Hanson, P. J.,
1086 Iversen, C. M. and Chanton, J. P.: Organic matter transformation in the peat column at Marcell
1087 Experimental Forest: Humification and vertical stratification, *JGR Biogeosciences*, (661–675),
1088 doi:10.1002/2013JG002492, 2014.
- 1089 Tfaily, M. M., Chu, R. K., Tolić, N., Roscioli, K. M., Anderton, C. R., Paša-Tolić, L., Robinson,
1090 E. W. and Hess, N. J.: Advanced Solvent Based Methods for Molecular Characterization of Soil
1091 Organic Matter by High-Resolution Mass Spectrometry, *Anal. Chem.*, 87(10), 5206–5215,
1092 doi:10.1021/acs.analchem.5b00116, 2015.
- 1093 Tfaily, M. M., Chu, R. K., Toyoda, J., Tolić, N., Robinson, E. W., Paša-Tolić, L. and Hess, N. J.:
1094 Sequential extraction protocol for organic matter from soils and sediments using high resolution
1095 mass spectrometry, *Anal. Chim. Acta*, 972, 54–61, doi:10.1016/J.ACA.2017.03.031, 2017.
- 1096 Tolić, N., Liu, Y., Liyu, A., Shen, Y., Tfaily, M. M., Kujawinski, E. B., Longnecker, K., Kuo,
1097 L.-J., Robinson, E. W., Paša-Tolić, L. and Hess, N. J.: Formularity: Software for Automated
1098 Formula Assignment of Natural and Other Organic Matter from Ultrahigh-Resolution Mass
1099 Spectra, *Anal. Chem.*, 89(23), 12659–12665, doi:10.1021/acs.analchem.7b03318, 2017.
- 1100 Trivedi, P., Delgado-Baquerizo, M., Trivedi, C., Hu, H., Anderson, I. C., Jeffries, T. C., Zhou, J.
1101 and Singh, B. K.: Microbial regulation of the soil carbon cycle: evidence from gene–enzyme
1102 relationships, *ISME J.*, 10(11), 2593–2604, doi:10.1038/ismej.2016.65, 2016.
- 1103 Tzortziou, M., Neale, P. J., Megonigal, P., Pow, C. L. and Butterworth, M.: Spatial gradients in
1104 dissolved carbon due to tidal marsh outwelling into a Chesapeake Bay estuary, *Mar. Ecol. Prog.
1105 Ser.*, 426, 41–56, doi:10.3354/meps09017, 2011.
- 1106 U.S. DOE.: Research Priorities to Incorporate Terrestrial-Aquatic Interfaces in Earth System
1107 Models: Workshop Report, DOE/SC-0187, 2017.
- 1108 Vidon, P., Allan, C., Burns, D., Duval, T. P., Gurwick, N., Inamdar, S., Lowrance, R., Okay, J.,
1109 Scott, D. and Sebestyen, S.: Hot Spots and Hot Moments in Riparian Zones: Potential for
1110 Improved Water Quality Management ¹, *JAWRA J. Am. Water Resour. Assoc.*, 46(2), 278–298,
1111 doi:10.1111/j.1752-1688.2010.00420.x, 2010.
- 1112 van der Wal, A., Ottosson, E. and de Boer, W.: Neglected role of fungal community composition
1113 in explaining variation in wood decay rates, *Ecology*, 96(1), 124–133, doi:10.1890/14-0242.1,

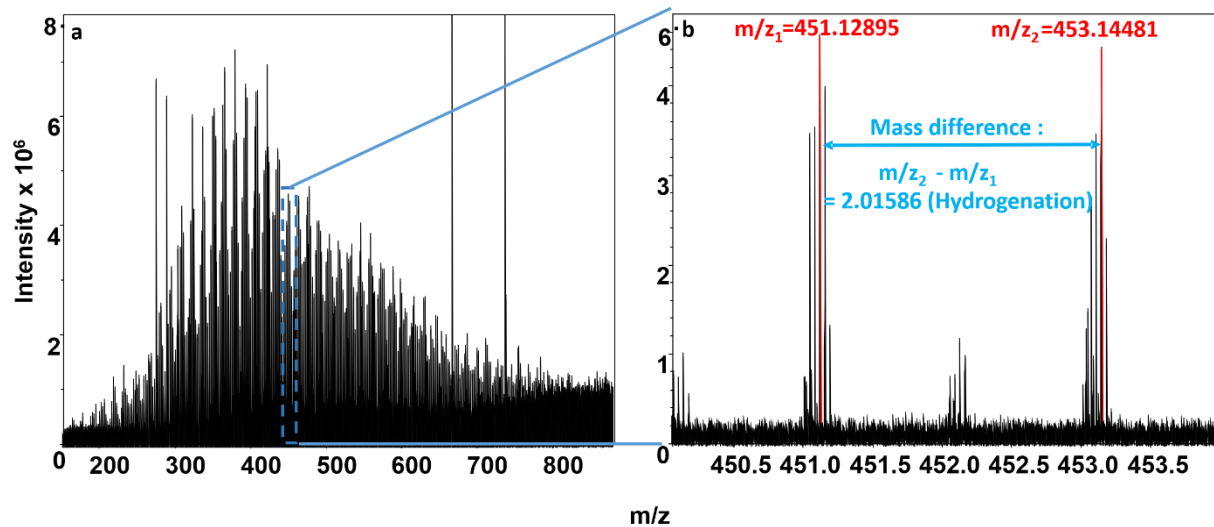
- 1114 2015.
- 1115 Ward, C. P., Nalven, S. G., Crump, B. C., Kling, G. W. and Cory, R. M.: Photochemical
1116 alteration of organic carbon draining permafrost soils shifts microbial metabolic pathways and
1117 stimulates respiration, , doi:10.1038/s41467-017-00759-2, 2017a.
- 1118 Ward, N. D., Keil, R. G., Medeiros, P. M., Brito, D. C., Cunha, A. C., Dittmar, T., Yager, P. L.,
1119 Krusche, A. V. and Richey, J. E.: Degradation of terrestrially derived macromolecules in the
1120 Amazon River, *Nat. Geosci.*, 6(7), 530–533, doi:10.1038/ngeo1817, 2013.
- 1121 Ward, N. D., Bianchi, T. S., Medeiros, P. M., Seidel, M., Richey, J. E., Keil, R. G. and
1122 Sawakuchi, H. O.: Where Carbon Goes When Water Flows: Carbon Cycling across the Aquatic
1123 Continuum, *Front. Mar. Sci.*, 4(January), doi:10.3389/fmars.2017.00007, 2017b.
- 1124 Ward, N. D., Indivero, J., Gunn, C., Wang, W., Bailey, V. and McDowell, N. G.: Longitudinal
1125 gradients in tree stem greenhouse gas concentrations across six Pacific Northwest coastal forests,
1126 *J. Geophys. Res. Biogeosciences*, 2019JG005064, doi:10.1029/2019JG005064, 2019a.
- 1127 Ward, N. D., Morrison, E. S., Liu, Y., Rivas-Ubach, A., Osborne, T. Z., Ogram, A. V. and
1128 Bianchi, T. S.: Marine microbial community responses related to wetland carbon mobilization in
1129 the coastal zone, *Limnol. Oceanogr. Lett.*, 4(1), 25–33, doi:10.1002/lol2.10101, 2019b.
- 1130 Washington Department of Fish and Wildlife: Fish Passage & Diversion Screening
1131 Inventory., 2019.
- 1132 Weston, N. B., Dixon, R. E. and Joye, S. B.: Ramifications of increased salinity in tidal
1133 freshwater sediments: Geochemistry and microbial pathways of organic matter mineralization, *J.*
1134 *Geophys. Res.*, 111(G1), G01009, doi:10.1029/2005JG000071, 2006.
- 1135 Weston, N. B., Vile, M. A., Neubauer, S. C. and Velinsky, D. J.: Accelerated microbial organic
1136 matter mineralization following salt-water intrusion into tidal freshwater marsh soils,
1137 *Biogeochemistry*, 102(1–3), 135–151, doi:10.1007/s10533-010-9427-4, 2011.
- 1138 Weston, N. B., Neubauer, S. C., Velinsky, D. J. and Vile, M. A.: Net ecosystem carbon exchange
1139 and the greenhouse gas balance of tidal marshes along an estuarine salinity gradient,
1140 *Biogeochemistry*, 120(1–3), 163–189, doi:10.1007/s10533-014-9989-7, 2014.
- 1141 Yang, J., Zhan, C., Li, Y., Zhou, D., Yu, Y. and Yu, J.: Effect of salinity on soil respiration in
1142 relation to dissolved organic carbon and microbial characteristics of a wetland in the Liaohe
1143 River estuary, Northeast China, *Sci. Total Environ.*, 642, 946–953,
1144 doi:10.1016/J.SCITOTENV.2018.06.121, 2018.
- 1145 Zark, M. and Dittmar, T.: Universal molecular structures in natural dissolved organic matter.,
1146 *Nat. Commun.*, 9(1), 3178, doi:10.1038/s41467-018-05665-9, 2018.
- 1147 **Table 1.** Relative peak abundances (%) of compound classes in the water extracted organic
1148 carbon fraction averaged across replicates per site. Samples are ordered according to their depth
1149 profile (shallow and deep) and their relative position in the landscape: floodplain (Fp), inland (I),
1150 and upland (U). Abbreviations: Con HC (condensed hydrocarbon), UnsatHC (unsaturated
1151 hydrocarbon), Other (no classification assigned)

Site/Depth	Landscape position	Protein	Amino Sugar	Lipid	Lignin	Con HC	Tannin	Other	Carb	Unsat HC
BC2_Shallow	Fp	17.2	3.3	9.4	31.0	22.3	13.2	0.5	1.8	1.3
BC3_Shallow	Fp	21.6	3.8	11.5	27.3	23.0	9.8	0.4	1.5	1.2
BC4_Shallow	I	1.6	0.6	0.3	45.3	32.2	18.9	0.04	0.8	0.2
BC12_Shallow	Fp	7.6	1.8	4.0	38.1	31.2	15.3	0.1	1.2	0.7
BC13_Shallow	Fp	13.3	2.6	5.9	33.4	28.6	14.4	0.2	0.9	1.0
BC14_Shallow	I	6.1	1.7	1.6	37.0	35.8	16.	0.2	0.8	0.5
BC15_Shallow	U	3.7	1.5	1.3	51.8	18.5	21.0	0.2	1.5	0.5
BC2_Deep	Fp	2.3	0.5	1.5	41.2	27.2	25.7	0.2	1.1	0.3
BC3_Deep	Fp	3.2	0.3	3.1	34.1	33.4	24.4	0.3	0.9	0.2
BC4_Deep	I	2.8	0.8	0.6	50.4	27.7	16.5	0.2	0.7	0.2
BC12_Deep	Fp	2.29	0.40	1.43	43.3	27.9	22.9	0.2	1.2	0.3
BC13_Deep	Fp	3.47	0.62	2.00	39.8	33.6	19.2	0.2	0.8	0.3
BC14_Deep	I	1.71	0.76	0.57	43.7	32.5	19.34	0.2	1.0	0.2
BC15_Deep	U	9.51	2.55	4.70	63.8	5.1	9.93	0.7	1.0	2.6

1152



1153
 1154 **Figure 1.** Study site Beaver Creek in the Olympic Peninsula in western Washington. The creek
 1155 is a first order stream with tidal exchange restored in 2014. Top panel shows site location in
 1156 western Washington with inset panel zoomed in to show site close to Johns River. Bottom panel
 1157 shows soil sampling locations at the high salt exposure (BC2, BC3, BC4) transect, moderate salt
 1158 exposure (BC12, BC13, BC14) transect, and terrestrial upland (BC15) site. The transects with
 1159 six sampling sites experience periodic inundation episodes which result in surface pooling of
 1160 tidal water. Map was created using ArcGIS 10.5 software (ESRI, 2017). Coordinate System:
 1161 GCS WGS 1984.



1162

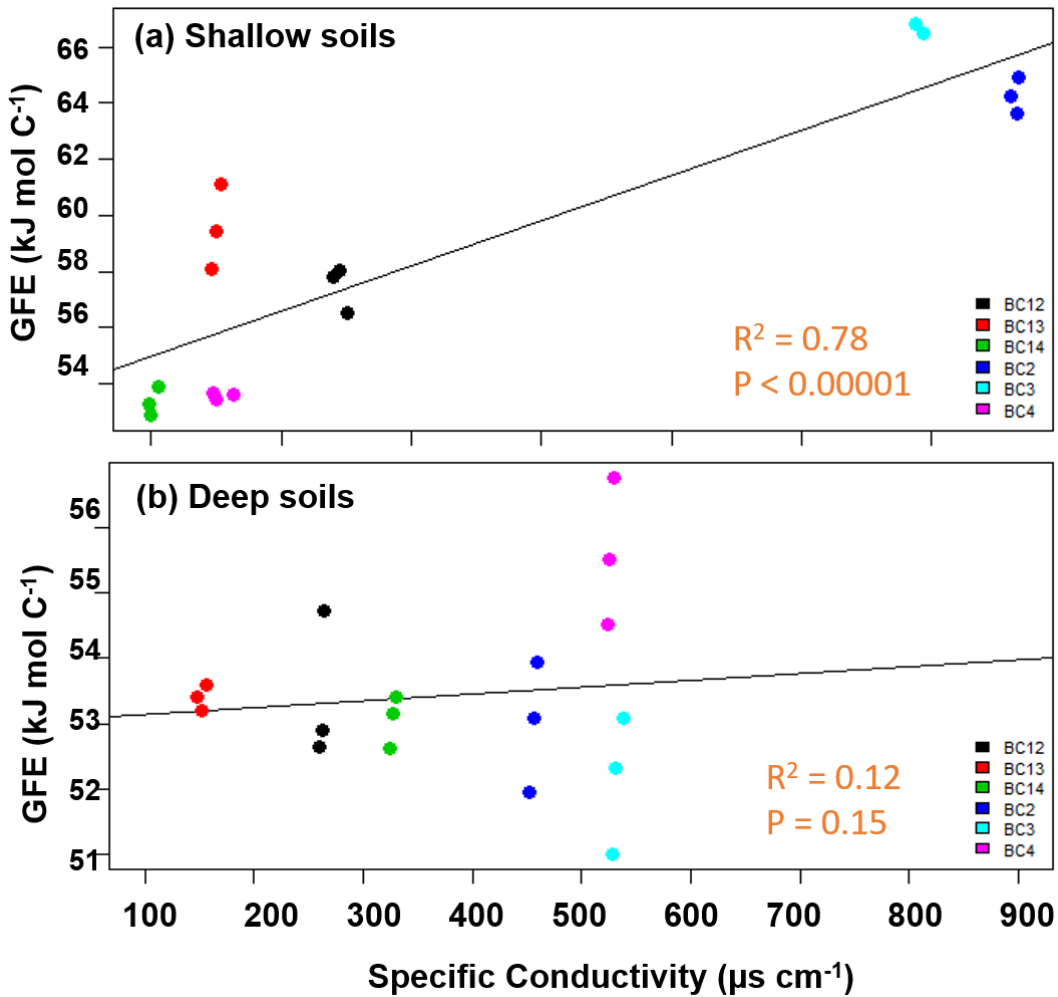
1163

1164 **Figure 2.** a) Negative mode FTICR-MS (full spectrum); b) zoom in at ~ 450 m/z showing an

1165 example of our FTICR-MS spectra overlain with peak mass assignments (red), and a

1166 biochemical transformation (mass difference between peaks, denoted in blue). Y axis denotes

1167 peak intensities, X-axis denotes mass-to-charge ratio.



1168

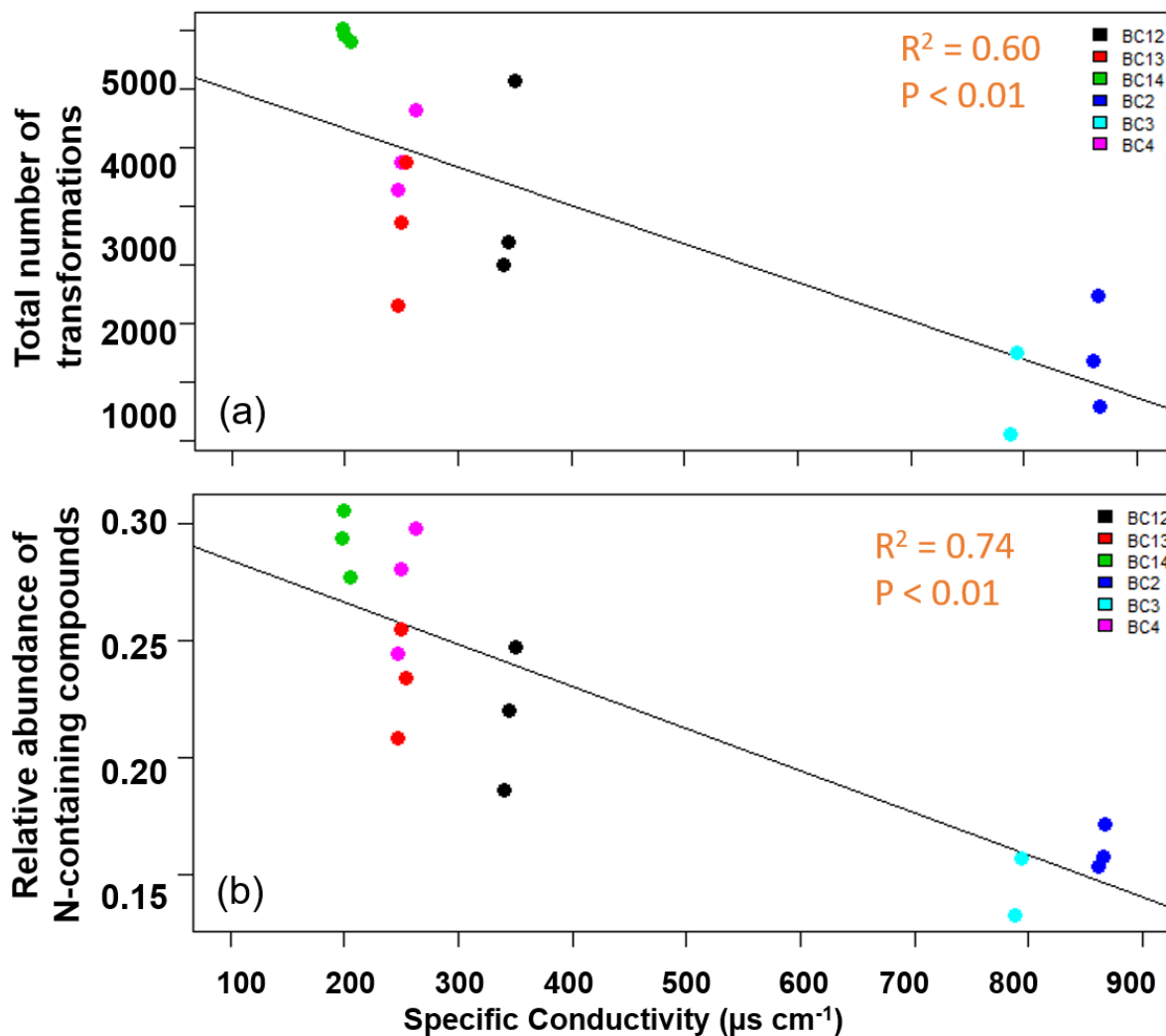
1169 **Figure 3.** Average Gibbs Free Energy (GFE) of samples in the water fraction of shallow soils
 1170 impacted by tidal inundation increased with increasing specific conductivity (a) while no change
 1171 was observed in the deeper soils (b). The salinity of the soil samples did not follow a clear spatial
 1172 gradient.

1173

1174

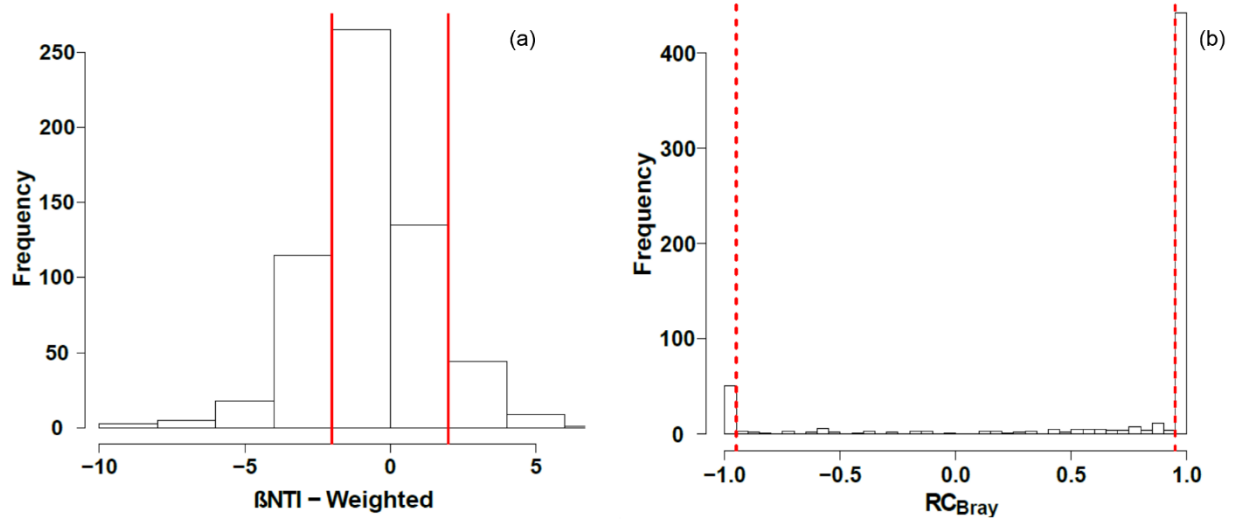
1175

1176



1177
 1178 **Figure 4.** The total number of inferred transformations (a) and total abundance of N-containing
 1179 compounds (b) in the water fraction of shallow soils impacted by tidal inundation show
 1180 significant negative correlations with increasing specific conductivity. No significant
 1181 relationships were observed for water fraction of deeper soils or for the CHCl_3 fraction in
 1182 shallow or deeper soils. The salinity of the soil samples did not follow a clear spatial gradient.

1183
 1184
 1185



1186

1187 **Figure 5.** Histograms representing the observed distribution of comparisons based on (a) Beta-
 1188 near taxon index (β NTI) and (b) Raup Crick metric (RC_{Bray}). Red lines represent the significance
 1189 thresholds, whereby values outside their bounds are significantly different from the null
 1190 distribution.

1191

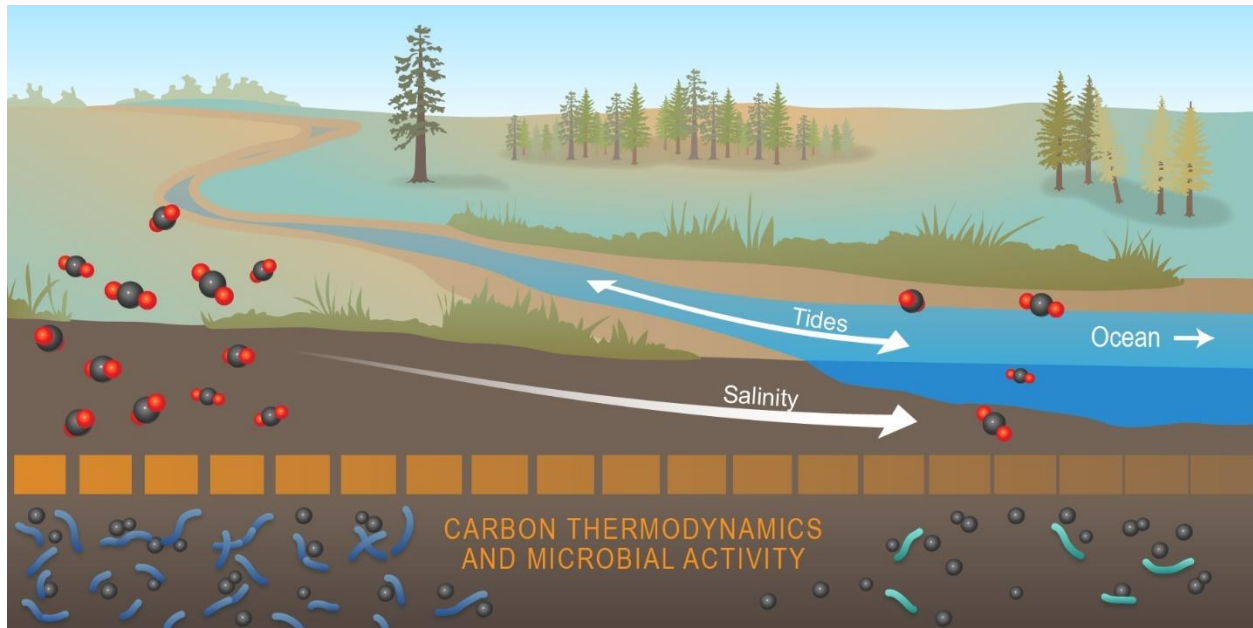
1192

1193

1194

1195

1196



1197

1198 **Figure 6.** Conceptual model summarizing the key outcome of our study: Microbial activity at
1199 high salinity may be depressed by thermodynamically less favorable C. Collectively, our data
1200 revealed that organic C thermodynamic favorability, heteroatom content, and number of
1201 biochemical transformations all decreased with increasing salinity. This suggest that microbial
1202 activity was lower at higher salinity, and we hypothesize this was due to lower thermodynamic
1203 favorability of organic C. To evaluate generality, the salinity-associated gradients shown here
1204 need to be evaluated across coastal watersheds and mechanistically understood as they have
1205 implications for contemporary and future C cycling in coastal watersheds experiencing
1206 hydrologic disturbances (e.g., sea level rise and storm surge).